Università degli Studi di Ferrara

DOTTORATO DI RICERCA IN
"SCIENZE BIOMEDICHE E BIOTECNOLOGICHE"

CICLO XXXII

COORDINATORE Prof. Paolo PINTON

Antidepressants targeting the ubiquitin-proteasome-autophagy pathway increase mesothelioma response to chemotherapy

Settore Scientifico Disciplinare MED/04

PhD student

Dott.ssa Natascia Caroccia

Supervisors

Prof.ssa Carlotta Giorgi
Prof. Paolo Pinton

Anni 2017/2019

TABLE OF CONTENTS

ABBREVIATIONS

3-MA, 3-methyladenine;

aa, aminoacids;

ACE, angiotensin-converting enzyme;

ACE-I, angiotensin-converting enzyme inhibitors;

Ad, Adenovirus;

ADP, adenosine diphosphate;

AIF, apoptosis-inducing factor;

AIRTum, Italian Cancer Registry Association;

Akt, also known as Protein Kinase B;

AMPK, AMP-activated protein kinase;

ATG, autophagy related genes;

ATP, adenosine triphosphate;

Baf-A1, bafilomycin-A1;

BAP1, BRCA1-associated protein 1;

Bcl-2, B-cell lymphoma 2;

BK, bradykinin;

BRCA1, breast cancer type 1 susceptibility protein;

Ca^{2+}, calcium ions;

$[Ca^{2+}]$, Ca^{2+} concentration;

$[Ca^{2+}]_c$, cytosolic Ca^{2+} concentration;

$[Ca^{2+}]_{ER}$, endoplasmic reticulum Ca^{2+} concentration;

$[Ca^{2+}]_m$, mitochondrial Ca^{2+} concentration;

CABP, Ca^{2+}-binding protein;

CaM, calmodulin;

Cas3, Caspase-3;

ChT-L, chymotrypsin-like activity;

CQ, chloroquine;

Cyt c, cytochrome c;

cytAEQ, cytosolic aequorin;

CMA, chaperone-mediated autophagy;

Da, Dalton;

DAG, diacylglycerol;

$\Delta\psi_m$, mitochondrial membrane potential;

DIABLO, direct inhibitor of apoptosis-binding protein with low isoelectric point;

DMEM, Dulbecco's Modified Eagle Medium;

DNA, deoxyribonucleic acid;

EGFR, Epidermal Growth Factor Receptor;

EndoG, endonuclease G;

ER, endoplasmic reticulum;

$FADH_2$, flavin adenine dinucleotide;

FBXL2, F-box/LRR-repeat protein 2;

FBS, fetal bovine serum;

FDA, Food and Drug Administration;

FRET, fluorescence resonance energy transfer;

GAPDH, glyceraldehyde-3-phosphate dehydrogenase;

GFP, green fluorescent protein;

GPCR: G protein coupled receptor;

HM, human mesothelial cells;

HMGB1, high-mobility group box 1;

HtrA2, high temperature requirement protein A2;

IARC, International Agency for Research on Cancer;

IGF-1, insulin-like growth factor;

IMM, inner mitochondrial membrane;

IMS, intermembrane space;

IP_3, inositol 1,4,5-trisphosphate;

IP_3-BD, inositol 1,4,5-trisphosphate binding domain;

IP_3R, inositol 1,4,5-trisphosphate receptor;

LC3, microtubule-associated protein 1 light chain 3;

MAMs, mitochondria-associated membranes;

MEFs, mouse embryonic fibroblasts;

mETC, mitochondrial electron transport chain;

MCU, mitochondrial Ca^{2+} uniporter;

MFI, mean fluorescent intensity;

MM, malignant mesothelioma;

MPM, malignant pleural mesothelioma;

mtAEQ, mitochondrial aequorin;

mPTP, mitochondrial permeability transition pore;

mTOR, mammalian target of rapamycin;

MOMP, mitochondrial outer membrane permeabilization;

Na^+, sodium ions;

NADH, nicotinamide adenine dinucleotide;

NCX, Na^+/Ca^{2+} exchanger;

NF2, neurofibromatosis type 2;

OMM, outer mitochondrial membrane;

OXPHOS, oxidative phosphorylation;

PAS, phagophore assembly site;

PARP1, poly (ADP-ribose) polymerase 1;

PBS, phosphate buffered saline;

PDGF, Platelet-derived growth factor;

PGPH, peptidylglutamyl-peptide hydrolyzing activity;

PI3K, phosphatidylinositol 3-kinase;

PIP_2, phosphatidylinositol 4,5-bisphosphate;

PIP_3, phosphatidylinositol 3,4,5-trisphosphate;

PKA, Protein Kinase A;

PKB, Protein Kinase B,

PKC, Protein Kinase C;

PLC: phospholipase C;

PMCA, plasma membrane Ca^{2+}-ATPase;

PML, promyelocytic leukemia protein;

PtdIns, phosphatidylinositol;

PTEN, phosphatase and tensin homolog;

Raptor, regulatory-associated protein of mTOR;

RNA, ribonucleic acid;

ROS, reactive oxygen species;

RT-PCR, reverse transcriptase-polymerase chain reaction;

RyR, ryanodine receptor;

SCF, SKP1-CUL1-F-box protein E3 ligase;

SD, standard deviation;

SERCA, sarco/endoplasmic reticulum Ca^{2+}-ATPase;

shRNA, short hairpin RNA;

siRNA, short interfering RNA;

Smac, second mitochondria derived activator of caspase;

SR, sarcoplasmic reticulum;

SV40, simian virus 40;

T-L, trypsin-like activity;

TKR, tyrosine-kinase receptor;

TP53, gene encoding for tumour protein p53;

ULK1, unc51-like kinase 1;

UPS, ubiquitin-proteasome system;

VDAC, voltage-dependent anion channel;

VEGF, vascular endothelial growth factor;

VDCC: voltage-dependent Ca^{2+}channel

ABSTRACT

Malignant mesothelioma (MM) is a highly aggressive neoplasm with poor prognosis and survival averaging 6-12 months after diagnosis. The efficacy of the first-line treatment (pemetrexed plus *cis-platinum*) improves the overall survival of only 2-3 months because the marked resistance of MM cells to chemo-induced apoptosis limits response to the therapy. Recently, we demonstrated that the release of calcium (Ca^{2+}) from the endoplasmic reticulum (ER) to mitochondria, a crucial event in apoptotic cell death, is deregulated in MM cells. Similarly, different studies highlighted a pivotal role of the autophagic process in MM, wherein enhanced autophagy allows cells to survive cytotoxic stimuli, thus conferring cell death resistance. Here, we found that some antidepressants (ADs), DCMI and sertraline, and antipsychotics (APs), clozapine and haloperidol, presented anti-autophagic effects that increased apoptosis in MM cells treated with pemetrexed and *cis-platinum*, alone or in combination. Furthermore, we showed that in MM cells, autophagy induced the degradation of type III inositol 1,4,5-trisphosphate receptor (IP_3R3), the main player in Ca^{2+} release from ER to the cytosol and mitochondria, reducing apoptosis. By the other hand, ADs by inhibiting the autophagic-UPS (ubiquitin-proteasome system) degradation increased IP_3R3 levels, an effect that led to increased Ca^{2+} transfer from the ER to mitochondria and promoted apoptosis. In conclusion, our results suggest that the chemo-resistance in MM is largely related to reduced levels or activity of the IP_3R3 and consequent lower mitochondrial Ca^{2+} concentrations, which render cancer cells incapable to execute apoptosis. Thus, inhibiting the autophagic-UPS degradation of IP_3R3 in MM cells could stabilize the receptor and it could restore susceptibility to chemo-induced apoptosis. In this light, we propose that ADs and APs, in combination with chemotherapy drugs, could represent an interesting novel therapeutic strategy for MM.

INTRODUCTION

Chapter 1. Malignant mesothelioma: an overview

1.1 Tumour characteristics, epidemiological data and clinical outcome

Malignant mesothelioma (MM) is a rare and highly aggressive cancer whose incidence continues to increase worldwide [1]. It originates from the cells of the *mesothelium*, a tissue that covers, like a thin film, the surface of most of the internal organs. *Mesothelium* includes the pleura, the membrane that lines the lungs; the *peritoneum*, that lines the abdomen; the *pericardium*, the sac around the heart, and the *tunica vaginalis*, which lines the interior of the *scrotum* [2] (Fig.1). However, in most cases, mesothelioma developed in the pleura originating the malignant pleural mesothelioma (MPM).

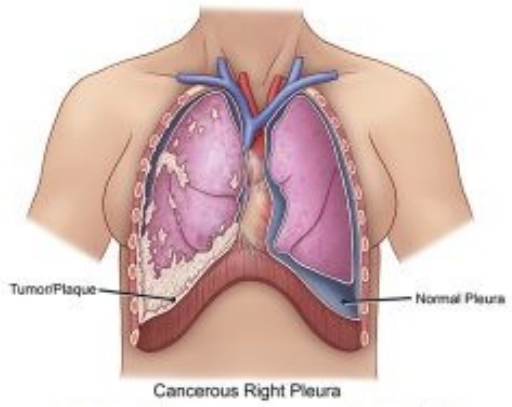

Figure 1. Malignant pleural mesothelioma (MPM).
Malignant mesothelioma (MM) is a rare and highly aggressive cancer that starts in the *mesothelium*, which includes the pleura, the thin layer of tissue that lines the lungs; the *peritoneum*, the membrane that lines the abdomen; and rarely the *pericardium*, the sac around the heart, and the *tunica vaginalis*, which lines the interior of the *scrotum*. Most cases of mesothelioma start in the pleura. This type of mesothelioma is also called malignant pleural mesothelioma (MPM). Mesothelioma almost always is caused by past exposure to fibers of asbestos. In rare cases, mesothelioma can be passed down from one generation to the next. Familial forms of MM are linked to germline mutations of several genes, mostly BRCA1-associated protein 1 (BAP1) gene.

Therefore, MM can originate in four different areas of the body: in the chest, in the abdomen and, very rarely, in the cavity around the heart and in the membrane that covers the testicles.

Benign tumours (adenomatous tumours, benign cystic mesothelioma, etc.) may also arise from the *mesothelium*, which are generally removed surgically and do not require further treatment [2,3]. Among all the forms of malignant mesothelioma, MPM is certainly the most common, accounting about 80% of all MMs [1].

MM is a male-predominant disease and, according to the Italian Cancer Registry Association (AIRTum), it represented 1% of all cancers affecting men and 0.2% of those diagnosed in women in Italy in 2019. Besides, 1800 new mesothelioma cases were estimated in 2019 (1300 in male subjects and 500 in female subjects) (P. Bironzo, F. Grosso and AIRTum Working Group, "Mesotelioma - I numeri del cancro in Italia 2019"). In the last few years, the number of cases is slightly increasing among women, probably because of the increasing number of female workers employed in the industrial production of materials containing asbestos, the main risk factor for this tumour [4]. In fact, MM is mainly associated with exposure to asbestos and, until a few years ago, this mineral was a widely used material in industry, thanks to its excellent soundproof properties, thermal, electrical and chemical resistance and great flexibility and versatility of use [5]. Remarkably, there are huge differences in the number of mesothelioma cases in different italian regions. For example, in the province of Alessandria, where there was an important industry for the production of materials containing asbestos, the incidence is above the national average with 16 cases per 100.000 for men and 13 cases per 100.000 for women [4].

The onset of mesothelioma is rare before 50 years old and has a maximum peak incidence around 70 years old. After diagnosis, 5-year survival rate is less than 20% in people between 45-54 years old and gradually decreases with advancing age [1]. Instead, in Italy, the estimated 5-year survival rate was less than 9% in 2019 [6,7].

1.2 Causes and risk factors

1.2.1 Exposure to asbestos and environmental risk factors

As already mentioned, the main risk factor for mesothelioma is asbestos exposure and its role in carcinogenesis has been known for over 50 years [8,9]. Most of MMs developed in people who have directly worked with this mineral or in its presence [10]. In addition, people who live in close contact with exposed workers are also at risk, since asbestos fibers can stick to clothes and be transported with them from work to home. Asbestos indicates a family of minerals, rather common in nature, with a very heat-resistant fibrous structure. The group consists of six naturally occurring fibrous minerals (chrysotile, amosite, crocidolite, tremolite, actinolite and anthophyllite) composed of thin, needle-like fibers, even more than a thousand times thinner than a human hair [11]. The small fibers that compose the minerals can be inhaled and can damage the mesothelial cells causing several cancers and diseases, including lung cancer [9], mesothelioma and asbestosis, a chronic disease characterized by scarring in the lungs, due to asbestos fibers deposited in the organ, which leads to long-term breathing complications. The International Agency for Research on Cancer (IARC) classifies all types of asbestos as carcinogens for humans, although a minor carcinogenic power is described for chrysotile respect to the others [11]. Therefore, these minerals are very dangerous to human health and, although there are asbestos strengthens and fireproof materials, they are banned in many countries. In Europe and in various developing countries, asbestos has been banned since 2005 but some nations, such as Russia, China, Kazakhstan, Brazil and Canada, still remain important producers. Interestingly, also exposure to other minerals, with similar fibers and physical characteristics to asbestos, like erionite (a naturally occurring fibrous mineral that belongs to a group of minerals called zeolites), could be a risk factor for the development of the MM [1,12].

Notably, there has not been reported so far a threshold value for asbestos amount that can be cause mesothelioma onset. However, a single fiber cannot cause cancer but a sufficient

"cumulative dose" is required. The risk increases with the amount of asbestos that has been inhaled and with the time exposure to the mineral. For this reason, the risk is very high in people who have worked in industries for the production or processing of objects containing asbestos but the required "cumulative dose" for the development of MM presents large variations between individuals [10]. Furthermore, it is important to remember that the latency time, which is the time that can elapse between the first exposure to asbestos and the onset of mesothelioma, is very long and can last up to 50 years [10]. In addition, the risk does not decrease once the exposure is completely eliminated, but remains constant throughout life.

1.2.2 Genetic risk factor

Although the exposure to asbestos is a major risk factor for mesothelioma, having been exposed to this mineral does not necessarily mean to develop the disease as, on the other hand, having not been exposed does not imply the certainty of never be affected by this form of cancer. In fact, 90% of the MM is caused by the exposure to asbestos, but only 5% of exposed people developed MM [1]. These observations indicate that there are also other causes for the onset of mesothelioma, even without occupational asbestos exposure. Indeed, rare familial forms of MM have also been described [13,14], which are linked to germline mutations of several genes (such as BRCA1-associated protein 1, *BAP1*) that can be transmitted from one generation to another [13,15,16]. BAP1 is a deubiquitinating enzyme with several roles in regulating deoxyribonucleic acid (DNA) repair, histone modification and gene expression and its dysfunction induces alterations in global gene expression profiling [17,18]. In the last decade, many studies have shown that polymorphism in the genes involved in oxidative metabolism or in DNA repair processes may play an important role in the pathogenesis of these diseases [19]. Indeed, molecular genetic analysis on MM patients have identified several genetic alterations, which are responsible for the development and progression of MM and are potential targets for molecular targeted therapy [20]. The loss of various tumour suppressor

genes was identified as the most common molecular event in MM [21]. Most frequently mutated tumour suppressor genes are the cyclin-dependent kinase inhibitor 2A/alternative reading frame (*CDKN2A/ARF*), neurofibromatosis type 2 (*NF2*), the already cited *BAP1* and occasionally the tumour protein p53 (*TP53*) genes [13,17]. A recent comprehensive genomic analysis has confirmed that recurrent gene fusions and splice alterations are frequent mechanisms for inactivation of *NF2* and *BAP1* in these diseases and their alteration are relatively characteristic of MM [13]. Notably, Merlin, which is encoded by *NF2*, regulates multiple cell signalling cascades including the Hippo and mammalian target of rapamycin (mTOR) pathways, which regulate important cell functions such as cell proliferation and growth. Through integrated analyses, alterations in Hippo, mTOR, histone methylation, ribonucleic acid (RNA) helicase and p53 signalling pathways have also identified in MM [22]. The discovery of familial cancer syndromes with germline mutations of these tumour suppressor genes also indicates the importance of genetic factors in MM predisposition. However, the genetics of MM susceptibility remains a relatively unexplored area.

The pathogenesis of MM has not yet been fully understood but seems to be related to the release of reactive oxygen and nitrogen species by macrophages. These molecules have mutagenic effects on DNA, with autocrine stimulation deriving from the activation of oncogenes (*MET*, *EGFR*, *PDGF*, *IGF-1*, *VEGF*) [20], the inactivation of tumour suppressor genes (as *BAP1*) [15] and the resistance to apoptosis [23].

1.2.3 Other risk factors

Other less common risk factors that have been reported to cause MM are thorax and abdomen ionizing radiation and exposure to Thorotrast10 (thorium dioxide, contrast medium used in radio-diagnostics until the 1950s) [24] and also, as reported in many studies, the simian virus 40 (SV40) infection [25-27]. Indeed, one of the most studied risk factor is SV40, which was

found to be able to cause mesothelioma in mice and has been found in some forms of human MM [27].

1.3 Diagnosis

Unfortunately, the formulation of a correct diagnosis is not easy and it often comes at an advanced stage of the disease when MM becomes more difficult to treat [6]. Indeed, the clinical symptoms are underestimated or misunderstood, since MM is a heterogeneous tumour and can be confused with other benign or malignant pathologies affecting the pleura. Furthermore, the diagnosis is hampered by the difficulty to correlate the symptoms with an exposure to a harmful carcinogenic substance that occurred many years ago. However, there are no screening methods that allow the early diagnosis of the disease in asymptomatic subjects, therefore the only real prevention that can be implemented today is to avoid exposure to asbestos and erionite.

1.4 Therapeutic strategies

Even with the current use of different therapeutic options, MM remains challenging to treat. Patients with MM have poor outcomes because multimodality treatments are suboptimal and currently no therapy is curative. Indeed, MM is largely unresponsive to chemotherapy and refractory to conventional therapies even with a combination of aggressive surgical intervention, radiation therapies and multimodality strategies. First line therapy is chemotherapy based on *cis-platinum* in combination with pemetrexed [28], drugs that induce apoptosis through unknown mechanisms, which have not yet been clearly defined. Because MM cells are largely resistant to apoptosis [23], the efficacy of *cis-platinum* and pemetrexed is limited, resulting only in 2-3 months improvement in median survival [7,29]. Nowadays, no validated treatment beyond standard front-line therapy is available. Combination of novel

drugs, such as the addition of bevacizumab (anti-VEGF antibody, an antiangiogenic compound) combined with *cis-platinum* plus pemetrexed, has shown some promise [30] but it should be noted that bevacizumab is not approved, at present, by the Italian Agency of drugs (AIFA) for this application. However, immunotherapy, specially immune checkpoint inhibitors, has generated a lot of excitement because of data suggesting the potential value of immune checkpoint inhibitors for patients who have failed chemotherapy but modern targeted therapies, or combination of novel drugs, that have been shown to be beneficial for other cancers have failed in MM so far [31]. More effective therapeutic strategies are therefore needed for MM [1,31].

Chapter 2. Ca^{2+} signalling and apoptotic cell death in cancer

2.1 Ca^{2+} as intracellular signal

Eukaryotic cells perceive and correctly respond to a wide range of extracellular signals, including hormones, growth factors, neurotransmitters and cell-cell interactions. Commonly, these extracellular inputs, through the interaction with cellular receptors harboring intrinsic enzymatic activity, coupled to intracellular effectors via G proteins or acting as ion channels, conveying the extracellular "message" in intracellular responses activating different signalling pathways. Frequently, the activated internal responses lead to the increase of the concentration of calcium ions (Ca^{2+}) in the cytoplasm with defined amplitude and kinetics that are used by the cell as intracellular signals for the regulation of multiple cellular processes [32]. Indeed, since life begins, Ca^{2+} mediates a plethora of different mechanisms, from the fertilization and regulation of the cell cycle events during the early developmental processes, to specific functions once the cells differentiate. In order to use Ca^{2+} as cellular messenger, cytosolic Ca^{2+} concentration $[Ca^{2+}]_c$ is maintained at very low levels in resting cells (~100 nM) and its intracellular distribution is highly and finely regulated. Consequently, controlled changes in intracellular Ca^{2+} levels provide dynamic and versatile signals permitting to use Ca^{2+} variations as pleiotropic messengers in the context of wide-ranging cellular events as diverse as gene expression, proliferation, cell death, motility, membrane trafficking, secretion, fertilization, development, muscle contraction and membrane excitability, and neuronal synaptic plasticity in learning and memory [32].

The universality of Ca^{2+} as intracellular messenger, capable of regulating such different processes, depends mainly on the spatio-temporal complexity of Ca^{2+} signals in terms of amplitude, duration, frequency and localization [32,33]. The formation of the correct spatio-temporal Ca^{2+} signals depends on a wide cellular machinery named the Ca^{2+} signalling toolkit, which includes several cellular Ca^{2+}-binding and Ca^{2+}-transporting proteins, present

mainly in the cytosol, plasma membrane, ER and mitochondria, and is continuously remodeled both in health and in disease [34,35] (Fig.2).

Since Ca^{2+} diffusion rates are slow and an extended intracellular stay of this cation is cytotoxic, cells have devised an ingenious mechanism of signalling to overcome the inherent problems connected to the features of Ca^{2+} and utilize it as second messenger, by presenting spatio-temporal changes in Ca^{2+} concentration. Indeed, single cell measurements have revealed that changes in Ca^{2+} levels can occur as repetitive brief spikes (Ca^{2+} oscillations) [36] or localized increases, confined or gradually propagate within the cells (Ca^{2+} waves) [32,33,37,38]. While rapid highly localized Ca^{2+} spikes regulate fast responses, repetitive global Ca^{2+} transients or Ca^{2+} waves manage slower reactions. To provide a very fast and effective Ca^{2+}-signalling, the cells use a huge amount of energy to maintain an almost 10000-fold Ca^{2+}-gradient between intracellular Ca^{2+} concentrations (~100 nM free) and extracellular environment (~1 mM) and internal stores, as endoplasmic reticulum (ER). However, to maintain this Ca^{2+} gradient, the cells compartmentalize, chelate or extrude Ca^{2+} from the cytoplasm to the outside milieu through active mechanisms by the plasma membrane Ca^{2+}-ATPase (PMCA) and the Na^{+}/Ca^{2+} exchanger (NCX) [34,39,40].

2.1.1 The Ca^{2+} signalling toolkit

In response to a wide range of stimuli, such as extracellular agonists, toxic stimuli, membrane depolarization, and stretch, intracellular [Ca^{2+}] increases through two fundamental mechanisms (or a combination of both). The first involves Ca^{2+} entry from the external milieu, through the opening of several plasma membrane Ca^{2+} channels, also driven by the electrochemical gradient existing between the two sides of the plasma membrane. These Ca^{2+}-entry channels display distinct features and their opening is triggered by different external signals, therefore they are traditionally grouped into three classes: voltage-dependent Ca^{2+}channels (VDCCs) [41], typical of excitable cells, receptor-operated Ca^{2+}

channels (ROCs) [42], for example the N-methyl-d-aspartate (NMDA) receptor that responds to glutamate, and second messenger-operated Ca^{2+} channels (SMOCs) [43] that respond to internal messengers. The second mechanism is the release of Ca^{2+} that is stored in intracellular compartments, mainly the ER and its specialized form in muscle, the sarcoplasmic reticulum (SR) [38]. Ca^{2+} release from internal stores can be modulated by Ca^{2+} itself, upon the entry of external Ca^{2+} induced by different stimuli, but also by the formation of second messengers, such as inositol 1,4,5-trisphosphate (IP_3) and cyclic adenosine diphosphate ribose (cADPr). The main Ca^{2+} release-channels, present in the intracellular stores, are the IP_3 receptors (IP_3Rs) [44,45] and the ryanodine receptors (RyRs) [46]. However, IP3Rs, present on the ER membrane, are the most ubiquitous. They are ligand-gated channels that release Ca^{2+} from ER Ca^{2+} stores, in response to the binding of their ligand, the second messenger IP_3, usually generated upon the activation of G protein coupled receptors (GPCRs) or tyrosine-kinase receptors (TKR). Indeed, GPCRs can activate phospholipase C (PLC)-β and TKR can activate PLC-γ, which then cleave phosphatidylinositol 4,5-bisphosphate (PIP_2) into IP_3 and diacylglycerol (DAG), both of which function as second messengers [47]. IP_3 binding to the IP_3Rs, causes efflux of Ca^{2+} from the ER to the cytoplasm resulting in increase in $[Ca^{2+}]_c$ from ~100 nM up to 1-3 μM for several seconds, activating various Ca^{2+}-dependent intracellular events [47]. Diverse cellular proteins with Ca^{2+}-binding affinities, ranging between nM to mM, are ubiquitous present in the cells to buffer the $[Ca^{2+}]_c$ increase as well as to regulate cellular processes via Ca^{2+}-signalling. Indeed, intracellular Ca^{2+} is predominantly bound to these buffers, whereas a small proportion binds to the effectors that activate different cellular processes. The correct cellular outcome depends on the spatio-temporal characteristics of the generated Ca^{2+} signal [32,33].

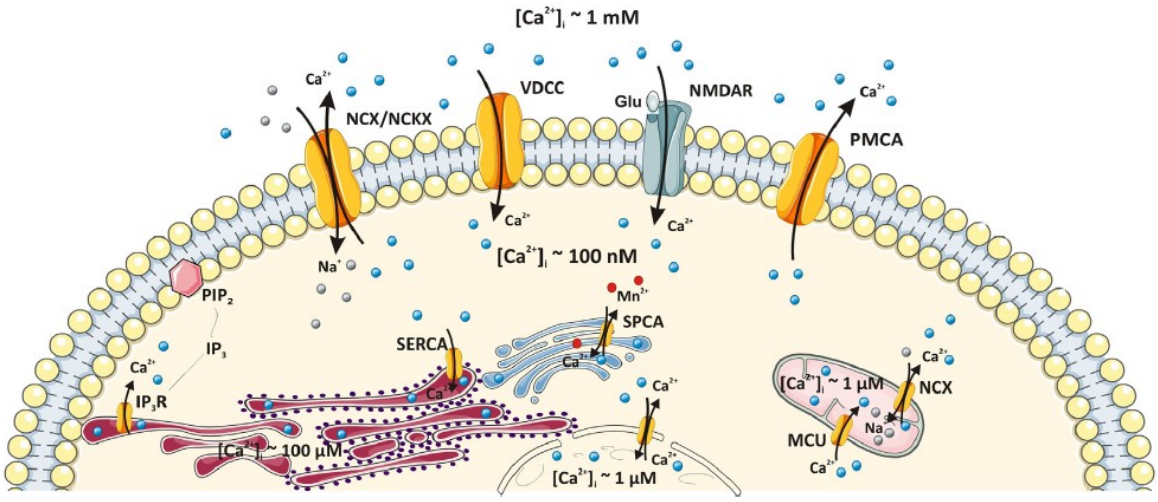

Figure 2. Schematic representation of Ca^{2+}circulation in the cell.

The universality of Ca^{2+} as an intracellular messenger depends on its enormous versatility. Cell have a Ca^{2+} signalling toolkit with many components, which includes several cellular Ca^{2+}-binding and Ca^{2+}-transporting proteins, present mainly in the cytosol, plasma membrane, endoplasmic reticulum (ER) and mitochondria that can be mixed and matched to create a wide range of spatial and temporal signals. Ca^{2+} enters into the cell through channels and pumps situated on the plasma membrane: VDCCs, typical of excitable cells, receptor-operated Ca^{2+} channels (ROCs) that responds to external messengers, e.g. NMDAR that responds to glutamate, and second messenger-operated Ca^{2+} channels (SMOCs) that respond to internal messengers (not shown). Various stimuli that act on cell surface receptors triggers the activation of phospholipase C (PLC) that catalyses the hydrolysis of PIP_2 to IP_3 and DAG. The binding of IP_3 to its receptor IP_3R stimulates ER Ca^{2+} release and consequently the transfer of Ca^{2+} from ER to mitochondria. Mitochondrial Ca^{2+} import occurs through its uniporter MCU. Ca^{2+} levels return to resting conditions through a series of channels and pumps: PMCA and NCX permit the ion extrusion into the extracellular milieu, SERCA (situated on the ER) and SPCA (on the Golgi apparatus) re-establish basal Ca^{2+} levels in intracellular stores. Abbreviations: **Glu**, glutamate; **IP_3**, inositol trisphosphate; **IP_3R**, inositol 1,4,5-trisphosphate receptor; **MCU**, mitochondrial Ca^{2+}uniporter; **NCKX**, Na^+/Ca^{2+}-K^+ exchanger; **NCX**, Na^+/Ca^{2+} exchanger; **NMDAR**, N-methyl-d-aspartate receptor; **PIP_2**, phosphatidylinositol 4,5-bisphosphate; **PMCA**, plasma membrane Ca^{2+}-ATPase; **SERCA**, sarco/endoplasmic reticulum Ca^{2+}-ATPase; **SPCA**, secretory-pathway Ca^{2+}-ATPase; **VDCC**, voltage-dependent Ca^{2+}channel (figure from [48]).

Once its downstream targets are activated, Ca^{2+} leaves the effectors and buffers and is removed from the cell by signal switching off mechanisms, in order to preserve the resting levels of Ca^{2+} and to refill internal stores. Hence, basal $[Ca^{2+}]_c$ levels are regained by the combined activity of Ca^{2+} extrusion mechanisms, such as multiple pumps and exchangers, PMCA and NCX [39,49], which extrude Ca^{2+} from cytosol to the external milieau, and mechanisms that refill the intracellular stores, like sarco/endoplasmic reticulum Ca^{2+}-

ATPases (SERCAs) [34]. Since SERCAs activity and the presence of several intraluminal Ca^{2+}-binding proteins (CABPs) inside the ER, such as calnexin and calreticulin, this cellular compartment is able to accumulate Ca^{2+} up to 1 mM, whereas the free [Ca^{2+}] reaches ~100-700μM, resulting in an overall estimated ER Ca^{2+} concentration ($[Ca^{2+}]_{ER}$) equal to a 1000-10000-fold higher compared to the cytosol [50-52]. Furthermore, also mitochondria participate to the recovery process sequestering Ca^{2+} rapidly, inside the mitochondria, through its uniporter, the mitochondrial Ca^{2+} uniporter (MCU) [53] (Fig.2). Indeed, although the ER (and its specialized form in muscle, the SR) is the main intracellular Ca^{2+} store, almost all other organelles are involved in Ca^{2+} signalling such as the Golgi apparatus [54], mitochondria [53,55], lysosomes [56] and peroxisomes [57].

2.2 IP_3R: main player in calcium release from cellular store

ER represents the most extensive intracellular organelle and the main dynamic cellular store of Ca^{2+} ions, which can rapidly respond to a huge variety of external stimuli, making this organelle a key component of Ca^{2+} signalling pathway [58]. The ER Ca^{2+} signalling system is composed by channels and pumps, IP_3Rs, RyRs and SERCAs, but also by Ca^{2+}-buffering proteins, such as calnexin and calreticulin, and other accessory proteins including triadin, sorcin and phospholamban [59]. As previously mentioned, Ca^{2+} release from ER is mainly mediated by the ubiquitous integral membrane ligand-gated channels IP_3Rs [60]. Numerous extracellular stimuli, such as hormones, growth factors and neurotransmitters, can trigger downstream IP_3 generation and Ca^{2+} release from the ER store through the interaction with different cellular receptors and the following activation of diverse isoforms of PLC. In particular, GPCRs and TKRs can activate PLC-β and PLC-γ respectively, whereas Ras proteins induce PLC-ε activation and an increase in Ca^{2+} concentration stimulates PLC-δ [61,62]. Therefore, the activated phosphodiesterases trigger the hydrolysis of the membrane phospholipid PIP_2 in DAG and IP_3, both of which function as second messengers [47]. Whereas

DAG mainly affects the activity of the Protein Kinase C (PKC) isoforms, IP_3 diffuse in the cytosol and binds to the nonselective cationic channels IP_3Rs on the ER, causing their opening and Ca^{2+} release [62]. Besides the ER, IP_3 can also stimulate Ca^{2+} release from the nucleus, Golgi apparatus and secretory vesicles.

In mammalian cells, three isoforms of IP_3R have been identified (IP_3R1, IP_3R2 and IP_3R3) that are encoded by different genes and share 60-80% aminoacids (aa) sequence homology [63]. They present different agonist affinities and tissue distribution [64,65]. In particular, IP_3R2 has more IP_3 affinity than IP_3R1, and both are largely more sensitive than IP_3R3 [66]. Whereas, for the diversity of protein expression, IP_3R1 is the dominant isoform in neuronal cells and smooth muscle, while IP_3R2 is mainly present in skeletal and cardiac muscle and IP_3R3 has a widespread expression in all tissues.

IP_3Rs are glycoprotein receptors with a molecular weight of approximately 260 kDa. Functional receptors exist as tetramers, composed of four identical (homotetramers) or different (heterotetramers) IP_3R isoforms, each one containing a cytoplasmic N-terminus, a hydrophobic region containing 6 transmembrane (TM) helices, and a cytoplasmic C-terminus [67]. The N-terminal of the each subunit contains a proximal IP_3-binding domain (IP_3-BD), i.e. the minimal sequence sufficient for IP_3 binding, and a distal regulatory domain [68]. N-terminally to the IP_3-BD, aa ranging from 1 to 222 form a suppressor domain, which inhibits ligand binding reducing the global receptor IP_3 affinity [69]. Moreover, this region plays a critical role in coupling the ligand binding to the channel gating, since experimental evidences showed that IP_3R cannot function when the entire domain is removed, although IP_3 still correctly binds the receptor [70]. Interestingly, between the IP_3-BD and the pore of the channel, there is the regulatory domain, which mediates intramolecular interactions with other IP_3R domains as well as the association with other regulatory proteins. In particular, the modulatory domain contains many consensus sequences for the binding of several factors involved in IP_3R regulation, such as Ca^{2+}-binding protein calmodulin (CaM), CABP1,

adenosine triphosphate (ATP) and Caspase-3 (Cas3) [71]. Moreover, this region possess phosphorylation sites for numerous kinases, including pro-survival protein kinase Akt (also known as Protein Kinase B, PKB) [72], cAMP-dependent Protein Kinase A (PKA) [73], Ca^{2+}-calmodulin-dependent protein kinase II (CaMKII) [74], PKC [75], cGMP-dependent protein kinase (PKG) [76] and various protein tyrosine kinases [77], which can directly phosphorylate and modulate IP_3R activity [78]. At the end, C-terminal of each subunit is composed by a six transmembrane-spanning domain, which enables IP_3R to be embedded in the ER membrane, and plays also a crucial role in receptor tetramerization and channel Ca^{2+} conductance regulation [79,80].

IP_3Rs are distributed and organized within clusters along the ER membrane. Cooperative receptor activation, mediated by both IP_3 and Ca^{2+}, which basically act as channel co-agonists, allow the formation of local and long-range Ca^{2+} signals [32]. Indeed, brief opening of single IP_3R, at a discrete site, creates localized Ca^{2+} pulses, known as "sparks" or "puffs", that recruit neighboring IP_3Rs, through a process named Ca^{2+}-induced Ca^{2+} release (CICR), combining Ca^{2+} "puffs" in Ca^{2+} waves [81,82].

The Ca^{2+} release from ER is a nonlinear and cooperative process that begins when IP_3 binds to all four receptor sites on the IP_3R, one on each subunit of the tetramer, inducing the conformational change within the transmembrane region that leads to Ca^{2+}-binding site sensitization [83]. Finally, upon Ca^{2+} binding, the channel opens and release Ca^{2+} from the cellular store. Ca^{2+} can induce Ca^{2+} release from ER in a biphasic manner. Indeed, early studies showed that micromolar concentrations of Ca^{2+} could inhibit IP_3-mediated Ca^{2+} mobilization [84]. Whereas, lower concentrations were found to potentiate the effects of IP_3 on the receptor [85]. In addition, also Ca^{2+} inside the organelle is able to regulate the channel opening since it has been seen that an increase in $[Ca^{2+}]_{ER}$ enhances the sensitivity of IP_3R for its ligand, promoting also spontaneous Ca^{2+} release, in permeabilized hepatocytes. However, the nature of this direct regulation and the protein involved are still a matter of

debate [86]. Although IP_3 and Ca^{2+} are essential for IP_3R channel activation, other physiological ligands can finely modulate the Ca^{2+}-sensitivity of the channel [87]. For example, ATP can regulate IP_3R in a biphasic manner as well as Ca^{2+}: while at micromolar concentrations ATP exerts a stimulatory effect, in the millimolar range it inhibits the channel opening [88].

As previously mentioned, IP_3R activity is modulated by a huge variety of stimulators and inhibitors, as well as phosphorylation and dephosphorylation events, mainly acting on the N-terminal suppressor domain of the channel [78]. Besides these interactions, also IP_3R expression levels can be regulated within the cell. Most of these processes are Ca^{2+} dependent, but also Ca^{2+}-independent mechanisms or acting via specific drugs have been described. Whereas, at post-transcriptional level, IP_3Rs mRNA is modulated by microRNAs and IP_3R protein expression is finally determined by ubiquitylation events and consequently by proteasomal degradation via ER-associated degradation (ERAD) [89,90]. Notably, also proto-oncogenes and tumour suppressors, as the phosphatase and tensin homolog (PTEN), B-cell lymphoma 2 (Bcl-2), promyelocytic leukemia protein (PML) and the breast cancer type 1 susceptibility protein (BRCA1), can affect IP_3Rs activity decreasing and enhancing it, respectively.

2.3 Ca^{2+}-uptake in mitochondria

ER is tightly connected to mitochondria creating very dynamic platforms that are termed mitochondria-associated membranes (MAMs). These specialized structures, at the interface between the two organelles, have been identified as microdomains enriched in Ca^{2+} signalling factors, which enable to rapidly respond to physiological and pathological Ca^{2+} signals selectively conveyed by ER directly to mitochondria [91,92]. The tight spatial relationship between ER and mitochondria, and the capacity of the latter to quickly clear the high [Ca^{2+}] microdomain generated in the proximity of the IP_3R, makes mitochondria an

active player in Ca^{2+} buffering and a resulting controller of IP_3R function. The uptake of the Ca^{2+} ions into the mitochondrial matrix leads to an increase, in a few seconds, in mitochondrial Ca^{2+} concentration ($[Ca^{2+}]_m$) to values above 10 μM and in some cell types up to 500 μM [93-95]. Nevertheless, besides its essential role in the maintenance of the Ca^{2+} homeostasis, mitochondrial Ca^{2+} uptake also modulates a wide-range of crucial processes like cellular metabolism, secretory functions, proliferation, migration, cell survival and apoptosis [96].

This process have long been considered to take place only when $[Ca^{2+}]_c$ increases in a high-amplitude prolonged manner, *i.e.* in the Ca^{2+} overload that is observed in numerous pathological conditions, due to the low affinity of the mitochondrial Ca^{2+} uptake system under physiological stimulation ($[Ca^{2+}]_c$ rarely exceeds 2-3 μM) [97]. However, using a novel, genetically encoded chemiluminescent probe, aequorin, which allow dynamic, accurate and specific monitoring of the $[Ca^{2+}]$ within the matrix of mitochondria in living cells, Rizzuto, Pozzan and colleagues showed in 1992 that mitochondria undergo very fast and large increases in their matrix Ca^{2+} levels upon physiological stimulation [93,98]. In addition, similar results were also obtained with other tools that accumulate within the organelle like fluorescent indicators, as the positively charged Ca^{2+} indicator rhod-2 [94] and the more recently developed green fluorescent protein (GFP)-based fluorescent probes [99]. In light of these results and a large body of other experimental evidences, it is now generally accepted that the rapid uptake of Ca^{2+} into mitochondria rests in the strategic location of mitochondria close to the opening ER Ca^{2+} channels (in MAMs regions) or Ca^{2+} channels situated on the plasma membrane [91].

Mitochondria are organelles characterized by two structurally and functionally different membranes: an outer membrane (outer mitochondrial membrane, OMM) and an internal one (inner mitochondrial membrane, IMM), which define an intermembrane space (intermembrane space, IMS) between them, and a mitochondrial matrix inside the organelle.

OMM is similar to the ER membrane and mainly consists of phospholipids, proteins and cholesterol. This plain outer membrane is mostly soluble to ions and metabolites up to 3000 Daltons (Da) due to the presence of many non-selective channels termed porins. Whereas, IMM is not plain but characterized by particular invaginations called *cristae*, which enclose the mitochondrial matrix, and presents high selectivity to ions and metabolites [100]. Inner membrane ion-impermeability enable mitochondria to generate and preserve an enormous electrochemical gradient, which is used to promote the mechanism of oxidative phosphorylation (OXPHOS) that produce cellular ATP. In fact, mitochondria are the main site of ATP production and generally considered the powerhouse of the cell. Glucose converted to pyruvate by glycolysis and products from fatty acid metabolism are converted to acetyl-CoA, which enters the tricarboxylic acid (TCA) cycle wherein they are fully degraded to carbon dioxide (CO_2). More importantly, these enzymatic reactions generate reduced forms of nicotinamide adenine dinucleotide (NADH) and flavin adenine dinucleotide ($FADH_2$), which trigger the mitochondrial electron transport chain (mETC). The mETC is composed by five different protein complexes: NADH dehydrogenase (complex I), succinate dehydrogenase (complex II), ubiquinol-cytochrome c (cyt c) reductase (complex III), cyt c oxidase (complex IV) and F_1F_O-ATP synthase that constitutes the final enzyme (complex V). Electrons transferred from NADH and $FADH_2$, through these complexes, move along the respiratory chain storing the energy as a very large electrochemical protons (H^+) gradient across the IMM. Thus, the translocation by protein complexes of H^+, from mitochondrial matrix to IMS, creates a mitochondrial membrane potential difference, $\Delta\psi_m$ = -180 mV, negative inside. Consequently, H^+ are forced to re-enter the matrix mainly through complex V, which dissipate this electrochemical gradient coupling the proton driving force to the phosphorylation of adenosine diphosphate (ADP) into ATP, according to the chemiosmotic theory [101]. Besides ATP production, it has become

clear that mitochondria employ the dissipation of the proton gradient, generated by the respiratory complexes, also to accumulate cations into the matrix [53,102].

The uptake of the Ca^{2+} ions into the mitochondria, taking advantage of the enormous driving force related to the negative transmembrane mitochondrial potential, involves different transport systems responsible for the transport of Ca^{2+} across the outer and the inner mitochondrial membrane. In particular, the Ca^{2+} transfer is carried out by the mitochondrial porin of the outer membrane, the voltage-dependent anion channel (VDAC), and by MCU through the IMM. However, the key transporter involved in mitochondrial Ca^{2+} uptake is the MCU, a highly selective ion channel with low affinity for Ca^{2+}, which takes up Ca^{2+} in the micromolar range and it reaches saturation only at more than physiological $[Ca^{2+}]_c$ [103]. Indeed, the overexpression of MCU (once called "CCDC109A") has been shown to increase mitochondrial Ca^{2+} uptake, which strongly sensitizes cells to apoptotic stimuli, and, by the other hand, silencing of MCU, using short interfering RNA (siRNA), reduce specifically Ca^{2+} uptake in mitochondria [104,105]. Recently, MCU was shown to be a macromolecular complex composed by pore-forming and regulatory subunits [106]. This mitochondrial uniporter is located in the IMM and presents two putative transmembrane domains with the N- and C-terminus facing the mitochondrial matrix. The *MCU* gene is nuclear and located on chromosome 10. It encodes for a 40kDa protein, which comprises the target sequence to mitochondria, that is cleaved when the protein is imported into the organelle, and the mature 35kDa protein. The resulting MCU is expressed in all the tissues and is able to oligomerization, giving rise to a complex of higher molecular weight [105].

Among the MCU regulatory subunits, mitochondrial calcium uptake 1 (MICU1), also known as FLJ12684 or CBARA1, has a key role in the modulation of the complex. Indeed, MICU1 acts as a gatekeeper of the channel, stabilizing MCU complex in its closed state and cooperating to allow Ca^{2+} to accumulate inside the mitochondria. Silencing MICU1 has been reported to abolish mitochondrial Ca^{2+} entry in intact and permeabilized cells, and to

attenuate the metabolic coupling between cytosolic Ca^{2+} transients and activation of mitochondrial dehydrogenases [107]. In 2012, it was also identified another important regulator of MCU, CCDC90A, now called mitochondrial calcium uniporter regulator 1 (MCUR1), an integral membrane protein that binds to MCU and regulates ruthenium-red-sensitive MCU-dependent mitochondrial Ca^{2+} uptake [108]. Ablation of MCUR1 can disrupt OXPHOS reducing cellular ATP and activating AMP kinase-dependent pro-survival autophagy. In addition, a biphasic effect of Ca^{2+} on the MCU has been reported since, beyond a certain level, $[Ca^{2+}]_c$ increase inactivates the uniporter, preventing further Ca^{2+} uptake and avoiding an excessive accumulation of the cation in mitochondria [109].

In light of these evidences, it becomes clear the essential role of MCU complex in mitochondrial Ca^{2+} uptake and the maintenance of the normal cellular bioenergetics.

2.4 Apoptotic cell death

Through their numerous and different metabolic functions, mitochondria power life. Indeed, they are the main energy producers in the cell and Ca^{2+} uptake into mitochondria can also modulate matrix enzymes that are involved in a wide range of other crucial cellular processes like cellular metabolism, cell survival, proliferation, migration, contraction and secretory functions [96]. Paradoxically, mitochondria also have a central role in apoptotic cell death since the above processes must be accomplished within the context of Ca^{2+} being highly toxic [100,110]. In fact, exceeding its normal spatial and temporal boundaries can result in cell death, mainly through the activation of the apoptotic pathway [32].

Apoptosis is a tightly regulated, energy-dependent and efficient mechanism of cell death, which involve various cell signalling pathways. The apoptotic process is defined by an orchestrated collapse of the cell, cytoplasmic shrinkage, chromatin condensation, DNA and protein cleavage, nuclear fragmentation and formation of apoptotic bodies followed by phagocytosis by neighboring cells [111,112]. The apoptotic network components are usually

already translated and present in the cell, at defined sites, ready to be activated by a pro-apoptotic stimulus and quickly respond to the death signal. Numerous stimuli, from outside or inside the cell, can induce the activation of the apoptotic pathways, such as oxidative stress, DNA damage, treatment with cytotoxic drugs or irradiation, interruption in cell cycle signalling and death receptors activation [111]. Furthermore, also the absence of survival factors is enough to drive a cell into apoptosis. This process occurs through two types of pathways: the extrinsic apoptotic pathway, triggered by the binding of death receptor ligands (tumour necrosis factor, TNF, and Fas ligand) to their receptors, and the intrinsic apoptotic pathway, which involve mitochondria and requires the activity of specific enzymes (caspases) and regulatory proteins (such as the Bcl-2 related family) [112,113].

Upon induction of the intrinsic apoptotic pathway, initial stage is the mitochondrial outer membrane permeabilization (MOMP), which usually commits a cell to die triggering the mitochondrial release into the cytoplasm of cyt c and intermembrane space-resident pro-apoptotic factors, which include caspase-independent death effectors, such as nucleases and/or proteases, as well as caspase co-factors [114,115]. Cyt c is undoubtedly one of the main players in the pivotal events that initiate the intrinsic apoptotic pathway. Once released into the cytoplasm, this protein drives the rearrangement and heptaoligomerization of the apoptosis–protease activating factor 1 (Apaf-1) leading to the assembly of the apoptosome, a platform that activates pro-caspases in response to intrinsic cell death signals [116]. Each of these complexes can recruit up to seven pro-caspase molecules, leading to their proteolytic cleavage and consequent activation [117]. A significant number of other pro-apoptotic molecules, such as Smac/DIABLO (second mitochondria derived activator of caspase/direct inhibitor of apoptosis-binding protein with low isoelectric point), apoptosis-inducing factor (AIF), HtrA2 (high temperature requirement protein A2) and endonuclease G (EndoG), are contained into the IMS and released into the cytosol upon cell death signals. They activate apoptosis through different pathways: Smac/DIABLO and HtrA2 interact and inhibit the

cytosolic inhibitors of apoptosis proteins (IAPs), such as XIAP, cIAP-1 and cIAP-2. The IAPs are generally associate to pro-caspases, stabilizing them and preventing their activation. Thus, Smac/DIABLO and HtrA2 inhibition of these peptides induce caspase activation. Instead, AIF and EndoG translocate directly from IMS to the nucleus where they are thought to mediate chromatin condensation and DNA fragmentation [118].

Beyond question, the crucial event that initiate the apoptotic process is the OMM permeability. However, the precise molecular mechanism underlying the process is still controversial. Indeed, different models have been proposed. One model involves opening of the mitochondrial permeability transition pore (mPTP) [119]. mPTP opening can be triggered by various stimuli and leads to the loss of mitochondrial membrane potential, as ions equilibrate across the OMM, and consequent water entry and swelling of the mitochondrial matrix. The latter can result in OMM dysruption, thus leading to the non-specific release of proteins from the IMS [120]. The second model for MOMP appears to be regulated by members of the Bcl-2 family acting directly on the OMM. It has been proposed that Bax, a pro-apoptotic Bcl-2 family member, directly interacts with the adenine nucleotide translocator (ANT) and VDAC inducing mitochondria permeabilization. Another model suggests that the release of pro-apoptotic proteins exclusively depends on the dynamic interactions and balance between pro-apoptotic and pro-survival members of the Bcl-2 protein family. In this model, BH3-only proteins (such as Bid, Bim, Puma and Noxa) play a pivotal role in pro-apoptotic Bax and Bak activation that results in their homo-oligomerization within the OMM. Pro-apoptotic Bax and Bak proteins exist as inactive monomers, with Bax localized in the cytosol and Bak in the mitochondrial fraction. Upon apoptosis induction, Bax translocates to mitochondria where it homo-oligomerizes and inserts in the OMM. Similarly, also Bak undergoes a conformational change that induces its oligomerization at the OMM. This leads to the formation of a pore in the OMM, which triggers the permeabilization of the

membrane and subsequent release of apoptogenic proteins and programmed cell death accomplishment [115,121].

2.5 Remodelling of Ca^{2+} signalling machinery in cancer cells

Intracellular Ca^{2+} signalling is fundamental for the regulation of innumerable cellular processes including muscle contraction, hormone secretion, synaptic transmission, as well as proliferation and cell migration. However, increases in intracellular Ca^{2+} that exceed the normal spatial and temporal boundaries are cytotoxic and lead to programmed cell death [122]. Consequently, Ca^{2+} needs to be modulated in an appropriate manner to determine cell fate, and cell survival finely depends on Ca^{2+} homeostasis. If this balance is compromised, several pathological situations may ensue [123,124].

ER and mitochondria form a highly dynamic interconnected network within which they can control Ca^{2+} signalling. During normal signalling, there is a continuous flow of Ca^{2+} between these two organelles, mainly transferred from the ER to the mitochondria. The switch into a death signal depends on the amplitude of the mitochondrial Ca^{2+} signal and the coincidental presence of pro-apoptotic stimuli [124]. A wide number of cell death signals, such as arachinodic acid, ceramide and oxidative stress induced by H_2O_2 or menadione, triggers a progressive release of Ca^{2+} from the ER, which consequently induces a mitochondrial Ca^{2+} overload [125]. Because of their central role in Ca^{2+} release from ER stores, IP_3Rs are directly responsible of the massive and/or prolonged Ca^{2+} overload into mitochondria. The relevance of these receptors in Ca^{2+}-dependent cell death has been demonstrated by several studies that have shown that ablation or reduction of IP_3R expression significantly reduces agonist-induced mitochondrial Ca^{2+} uptake, resulting in apoptosis-resistant cells [126,127]. In this context, the three isoforms of the IP_3R appear to function in different manners since IP_3R1 has shown to predominantly mediate cytosolic Ca^{2+} mobilization, whereas IP_3R3 seems to play a preferential role in apoptotic Ca^{2+} signals transmission to mitochondria [128].

Interestingly, cell sensitivity to apoptosis correlates with the Ca^{2+} content of the ER. Numerous studies indicate that procedures that decrease the Ca^{2+} loading of the ER, such as genetic ablation of calreticulin (an ER Ca^{2+}-buffering protein) or overexpression of plasma membrane Ca^{2+} ATPases, protect cells from apoptotic cell death [129]. On the contrary, molecular tools that increase the ER Ca^{2+} loading, such as overexpression of calreticulin or SERCA, sensitize cells to apoptotic stress. Accordingly, also procedures that enhance the transfer of Ca^{2+} from the ER to mitochondria increase cell death [130].

Since ER and mitochondria play significant roles in the regulation of apoptosis as well as cell survival and proliferation, through Ca^{2+} signalling machinery, it is not surprising that many cancer cells take advantage of this system to limit pro-apototic Ca^{2+} signals during oncogenic transformation and cancer development. In fact, Ca^{2+} signalling proteins and organelles are emerging as additional cellular targets of various oncogenes and tumour suppressors [131]. In this context, cancer cells proliferate at higher rates and protect themselves from apoptosis modulating the expression or the activity of Ca^{2+} signalling components, which regulate many relevant processes during tumourigenesis, such as apoptotic sensitivity, proliferation, migration and cell invasion. A common strategy for cancer cells is to increase expression of anti-apoptotic members of the Bcl-2 protein family (Bcl-2 and Bcl-XL), or decrease expression of the pro-apoptotic BH3-only proteins (Bax or Bak), in order to protect themselves from apoptosis by modulating intracellular Ca^{2+} signals. Remarkably, in cancer cells, Bcl-2 protein family mainly affects ER-mitochondrial Ca^{2+} crosstalk. Indeed, the over-expression of the anti-apoptotic protein Bcl-2 reduces the Ca^{2+} content of the ER making the cells resistant to apoptosis [129]. Similarly, mouse embryonic fibroblasts deficient for the pro-apoptotic proteins Bax and Bak (double KO cells) were found to have a reduced ER Ca^{2+} content that results in decreased Ca^{2+} transfer to mitochondria and in a dramatic increase in cell death resistance [132]. Recently, it has been demonstrated that Bcl-2 forms a macromolecular complex with the IP_3Rs. This interaction seems to control IP_3R-mediated

Ca^{2+} flux, suppressing release of Ca^{2+} from ER stores and preventing pro-apoptotic Ca^{2+} signalling [133]. In this light, anti-apoptotic Bcl-2 proteins seem to be the main physiological inhibitors of IP_3Rs. Moreover, decreased levels of pro-apoptotic proteins Bax and Bak are inversely correlated with the amount of Bcl-2 bound to the IP_3R, Ca^{2+} leak from the ER and the phosphorylation status of the IP_3R suggesting that Bcl-2 may regulate ER Ca^{2+}-store content by modulating the phosphorylation status and the activity of the IP_3R. IP_3Rs possess many consensus sequences, in their modulatory domains, for phosphorylation by numerous kinases, including Akt and PKA. The phosphorylation event is inhibitory for IP_3Rs activity, decreasing IP_3-induced Ca^{2+} release from the ER and mitochondrial Ca^{2+}-uptake, upon stimulation with pro-apoptotic stimuli, and consequently leading to apoptosis resistance [134,135]. Interestingly, in human prostate cancer and other tumours, Akt is constitutively active and IP_3Rs are hyper-phosphorylated suggesting that cancer cells take advantage of the functional interaction between Akt and IP_3Rs to escape from apoptosis by limiting Ca^{2+}-dependent cell death signalling [72].

2.5.1 IP_3R3 degradation through the ubiquitin-proteasome system in cancer

Among the three mammalian IP_3R isoforms, type III IP_3R (IP_3R3) appears to be the major player in Ca^{2+}-dependent apoptosis. Recently, two important studies have identified and highlighted novel molecular mechanisms that limit mitochondrial Ca^{2+} overload to prevent cell death in cancer cells carrying out IP_3R3 degradation through the ubiquitin-proteasome system (UPS) [136,137].

Critical cellular processes, such as cell cycle transitions and cell death induction, are normally regulated by maintaining the appropriate intracellular levels of specific proteins. Since *de novo* protein synthesis is a comparatively slow process, protein levels are usually regulated by a faster process, the degradation. A major mechanism for protein degradation is the UPS system [138]. In this process, addition of long poly-ubiquitin chains targets proteins

for degradation/recycling by the 26S proteasome, a cylindrical organelle that recognizes ubiquitinated proteins and triggers their proteolytic cleavage. The addition of multiple ubiquitin monomers, an abundant and essential 9kDa protein that is conserved across evolution from yeast to man, is a three-step process, which comprises ubiquitin activation, substrate recognition and is mediated by a three-enzyme ubiquitination complex [139]. In summary, an ubiquitin-activating enzyme (E1) binds ubiquitin in an ATP-dependent manner. Ubiquitin is then transferred to an ubiquitin-conjugating enzyme (E2) that transiently carries ubiquitin until its conjugation with the ubiquitin ligase (E3). This enzyme finally mediates the ubiquitin transfer to an internal lysine on the target protein. The formation of a poly-ubiquitin chain constitutes then the protein degradation signal for the 26S proteasome [140]. However, ubiquitin can also be reversibly conjugated to some proteins to regulate their function, depending on the degree of ubiquitination [141]. The selectivity of the UPS system for a specific substrate relies on the interaction between the E2 enzyme and the ubiquitin-ligase E3. While just a few ubiquitin-conjugating enzymes E2 are present in the cell, there are possibly hundreds of E3 ubiquitin ligases. Among them, the SCF (SKP1-CUL1-F-box protein) E3 ligases are the largest family and are responsible for the turnover of several regulatory proteins involved in many key cellular processes [142].

The first mentioned study showed that the F-box protein FBXL2 (F-box/LRR-repeat protein 2), the receptor subunit of one of 69 human SCF E3 ligases, is directly involved in IP_3R3 ubiquitin-mediated degradation through the proteasome pathway [136]. In this study, the authors demonstrated that FBXL2 binds IP_3R3 and targets it for protein degradation through the UPS system in order to limit Ca^{2+} influx into mitochondria. Indeed, FBXL2-knockdown cells and FBXL2-insensitive IP_3R3 mutant knock-in clones display increased cytosolic Ca^{2+} release from the ER and sensitization to Ca^{2+}-dependent apoptotic stimuli. Interestingly, the authors also found PTEN competes with FBXL2 for IP_3R3 binding, and the FBXL2-dependent degradation of IP_3R3 is increased in *Pten*$^{-/-}$ mouse embryonic fibroblasts (MEF)

and PTEN-null cancer cells. Remarkably, *Pten*$^{-/-}$ is a common genotype in human tumours and syndromes that predispose individuals to cancer. Furthermore, experiments using a new compound called GGTi-2418, a geranylgeranyl transferase inhibitor, which could prevent the interaction between FBXL2 and IP_3R3, has been shown that xenotransplanted tumours can be sensitized to photodynamic therapy, which is based on the ability of photosensitizer agents to cause Ca^{2+}-dependent cytotoxicity after irradiation with visible light. Thus, this evidence indicates that the molecule could stabilize IP_3R3, leading to an increased cytosolic Ca^{2+} release from the ER and a major sensitization to Ca^{2+}-dependent apoptotic stimuli [136]. Whereas, in the second study, the researchers have identified another protein, BAP1, as a master regulator of Ca^{2+}-induced apoptosis through the regulation of the IP_3R3 ubiquitination and degradation [137]. BAP1 is a potent tumour suppressor gene that regulates gene environment interaction in human carcinogenesis. Carriers of mutations in *BAP1* gene presents a high incidence of cancers, mostly malignant mesothelioma. Indeed, more than 60% of MMs carry *BAP1* mutations [143]. In this work, the authors demonstrated that BAP1 localizes at the ER wherein it can bind, deubiquitylates and stabilizes IP_3R3, allowing Ca^{2+} transfer from the ER to mitochondria promoting apoptosis. Reduced levels of BAP1 cause reduction both of IP_3R3 levels and of ER Ca^{2+} flux to mitochondria, preventing apoptotic cell death. Consequently, a higher number of cells exposed to genotoxic stress such as ionizing or ultraviolet radiation, or to asbestos, could survive, resulting in a higher rate of tumoral transformation. Furthermore, using mesothelioma cell lines and primary cultures obtained from MM-affected patients, our research group demonstrated that a critical dysregulation in Ca^{2+} signalling is present in mesothelioma. This feature has been associated with resistance to apoptotic stimuli and, of considerable interest, correction of intracellular Ca^{2+} signalling resulted in the rescue of efficient apoptotic responses through mitochondrial Ca^{2+}-uptake [144].

In light of this, it becomes clear that ER-mitochondria Ca^{2+} transfer is a key process for Ca^{2+}-dependent cell death signalling. Hence, modulation of targets that regulate $[Ca^{2+}]_{ER}$ and/or ER-mitochondrial Ca^{2+} transfer, such as IP_3R3 stabilization or inhibition of its degradation, could increase sensitization of tumour cells to apoptotic cell death, representing a valid therapeutic strategy for cancer.

Chapter 3. The autophagic pathway in mesothelioma

In addition to apoptosis, the ER-mitochondria Ca^{2+} signalling mediated by IP_3R3 can also modulate autophagy [145]. In response to environmental cues that promote IP_3 generation, IP_3Rs, located on the ER, allow Ca^{2+} transfer to mitochondria to promote oxidative phosphorylation. When Ca^{2+} entry into mitochondria decreased, it can result not sufficient for the activation of Kreb's cycle enzymes and the sustainment of the mitochondrial respiration, thus the autophagic process is induced as a survival mechanism to respond to the lack of energy production [146,147].

3.1 Autophagy

Autophagy is an evolutionarily conserved process of self-degradation of cellular components and organelles [148,149]. In eukaryotic cells, there are two different mechanisms that are responsible for degradation of cellular components: the already mentioned UPS system and autophagy. While the UPS system mediates only protein degradation, predominantly short-lived proteins, which are previously tagged by ubiquitin for the recognition by the 26S proteasome, the autophagic process is responsible for the degradation of cytosolic components and macromolecules, including long-lived proteins, and mediates the organelles turnover through the lysosomal degradation [150]. Although the UPS system and the autophagy were initially thought to be independent in substrate selectivity, components and action mechanisms, recent studies have highlighted a dynamic crosstalk and interplay between these two pathways of cellular degradation that share notable similarity in many aspects and functionally cooperate to maintain protein homeostasis [151]. However, there are mostly three types of autophagy: chaperone-mediated autophagy (CMA), micro- and macro-autophagy [152] (Fig.4). The latter two are evolutionary conserved ranging from yeast to man, whereas CMA is specific for mammals. CMA is a highly selective form of autophagy wherein

substrate proteins with the pentapeptide motif KFERQ, usually oxidized or misfolded proteins, are selectively targeted to lysosomes and translocated into the lysosomal lumen for degradation. CMA requires the tightly coordinated action of chaperones, such as the cytosolic heat-shock cognate protein HSC70, which carry target proteins, and a dedicated protein translocation complex, the lysosomal receptor LAMP2A, which is responsible of the protein translocation into the organelle [153]. Microautophagy is, instead, the direct uptake of soluble or particulate cellular constituents into lysosomes. Thus, the cytoplasmic substances are directly incorporated by lysosomal membranes and then degraded within the internal lumen. However, macroautophagy (hereafter referred as autophagy) is the most prevalent form of autophagy. This process requires the transient formation of double-membraned vesicles, called autophagosomes, for the cytoplasmic components sequestration and the subsequent fusion with lysosomes, wherein the enclosed materials are degraded by resident hydrolases [154].

3.1.1 The autophagic machinery

Autophagy is a five steps process that requires the concerted action of three core machinery complexes and other proteins. The pivotal discovery of autophagy-related genes (ATG), characterized in yeast and highly conserved from yeast to man, has provided a significant breakthrough in the understanding of this process [155]. Autophagy comprises the formation of the isolation membrane or phagophore (nucleation), elongation, membrane enclosure and autophagosome formation, autophagosome-lysosome fusion and finally lysosomal degradation (Fig.3-4).

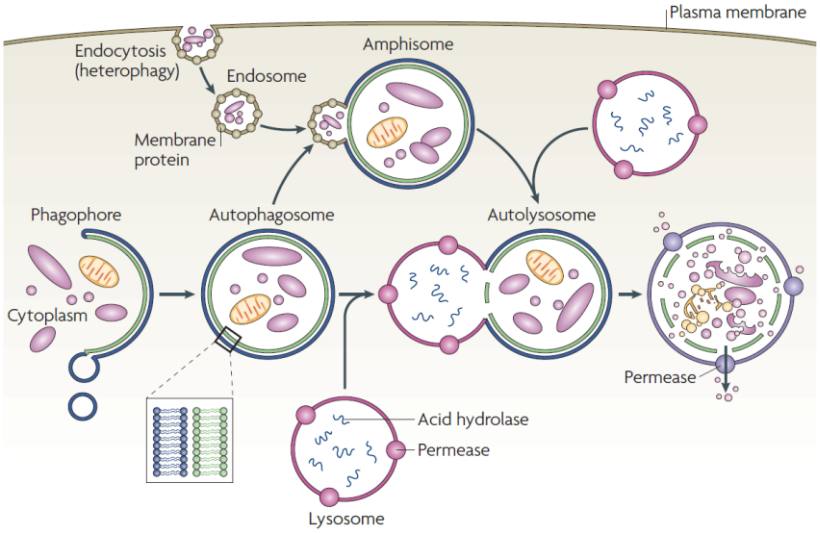

Figure 3. Schematic overview of the autophagic process.

Autophagy begins with the formation of the isolation membrane or phagophore (nucleation step). The process can engulf bulk cytoplasm nonspecifically, including entire organelles, or target cargos specifically. The concerted action of the autophagy core machinery proteins at the phagophore assembly site (PAS) is thought to lead to the expansion of the phagophore into an autophagosome (elongation step). When the outer membrane of the autophagosome fuses with an endosome (forming an amphisome before fusing with the lysosome) or directly with a lysosome (docking and fusion steps), it forms an autophagolysosome or autolysosome. Finally, the sequestered material is exposed to the lysosomal hydrolases and degraded inside the autophagolyosome (vesicle breakdown and degradation) and recycled (figure modified from [156]).

The induction of autophagy, that lead to the formation of the phagophore, is triggered by the ULK1 complex, composed by ULK1 (unc51-like kinase 1), the regulatory protein ATG13, RB1CC1/FIP200-C12orf44, and the ATG13-binding protein ATG101. The second autophagy core machinery complex is the class III phosphatidylinositol (PtdIns) 3-kinase (PI3K) complex, consisting of Beclin1, class III PI3KC3/VPS34, its regulatory protein kinase PI3KR4/VPS15/p150, AMBRA1 and ATG14/ATG14L/Barkor. It essentially exerts its role by the PI3K-III catalytic unit VPS34, which generates phosphatidylinositol 3,4,5-trisphosphate (PIP_3) that recruit a number of autophagy proteins involved in the nucleation of the autophagosome [157]. The integrated action of the core machinery proteins at the phagophore assembly site (PAS) leads to the expansion of the phagophore into an autophagosome (vesicle elongation) (Fig.4). Extension and closure of the autophagosome double membranes are mediated by two ubiquitin-like conjugation systems: the ATG12–

ATG5-ATG16L complex and the MAP1LC3/LC3-phosphatidylethanolamine (PE) conjugation system [158]. ATG7 and ATG10 enzymes covalently modify ATG5 with the ubiquitin-like protein ATG12 forming the ATG12-ATG5 conjugate, which is then stabilized by the interaction with the multimeric protein ATG16L. This complex is strictly required for the development of the autophagic membrane since it creates a coating surrounding the vacuole in formation and controls its curvature. Furthermore, ATG12–ATG5-ATG16L complex promotes the formation of the LC3-PE (LC3-II), the other conjugate essential for autophagosome formation. LC3 (microtubule-associated protein 1 light chain 3, a principal mammalian homologue of yeast ATG8) is a ubiquitin-like modifier synthesized in the pro-LC3 form, which is first processed by the cysteine protease ATG4 leading to LC3 (LC3-I) generation, and then covalently conjugated to PE by ATG7 (E1-like) and ATG3 (E2-like) enzymes through an ATP-dependent ubiquitin-like reaction, forming LC3-PE (LC3-II) [158]. This lipidated LC3-PE is then recruited on the newly forming autophagosome membranes. The conversion of the soluble form LC3-I to the lipidated LC3-II is thus well-known and widely used as a marker of autophagy activation [159]. After autophagosome formation, the LC3-II located in the outer site is released to the cytosol by ATG4 cleavage, whereas the LC3-II located in the inner site is degraded by lysosomal hydrolases. Remarkably, p62/SQSTM1, a cargo adaptor protein, which interacts with autophagic substrates and delivers them to autophagosome for lysosomal degradation, is itself degraded during the process. Thus, decrease in p62 levels indicates that autophagy has occurred, making p62 a suitable marker for autophagic degradation [160]. LC3-II localization on the phagophore is necessary for its elongation and final closure to form the mature autophagosome. Subsequently, autophagosome fuses with endosome forming amphisome, which undergoes a further fusion with lysosome generating autophagolysosome (or autolysosome) [161] (Fig.3 and Fig.4). Upon the fusion of its outer membrane with the lysosomal membrane, the

sequestered material as well as the inner membrane of the autophagosome are degraded to generate aminoacids and other cellular building blocks for recycling by the cell.

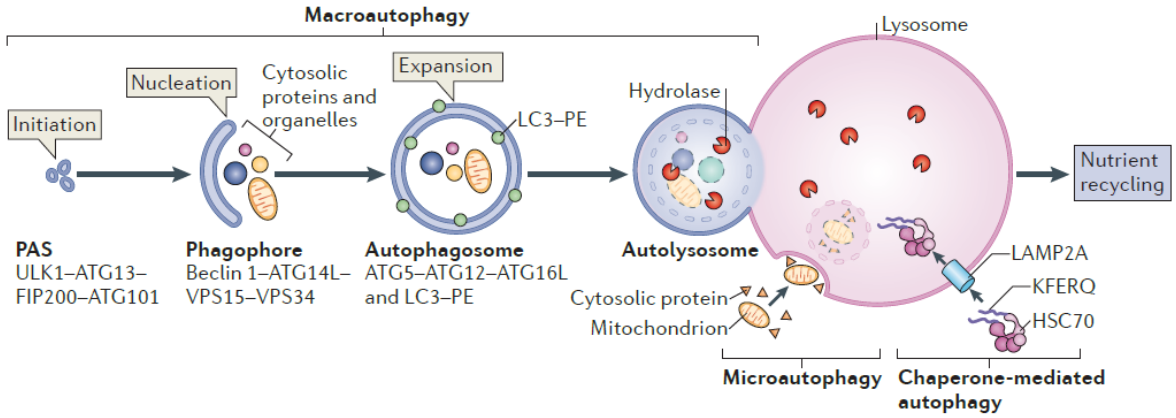

Figure 4. Overview of mammalian autophagy pathways.

In macroautophagy, initiation begins with the formation of the phagophore assembly site (PAS). This is mediated by the UNC51-like kinase (ULK) complex, which consists of ULK1, autophagy-related protein 13 (ATG13), FAK family kinase interacting protein of 200 kDa (FIP200) and ATG101. Further nucleation requires the class III PI3K complex, which is composed of the vacuolar protein sorting 34 (VPS34), along with its regulatory subunits ATG14L, VPS15 and Beclin1. Phagophore membrane elongation and autophagosome formation requires two ubiquitin-like conjugation pathways. The first produces the ATG5–ATG12 conjugate, which forms a multimeric complex with ATG16L, whereas the second results in the conjugation of phosphatidylethanolamine (PE) to LC3 (the microtubule-associated protein 1 light chain 3, ATG8 in yeast). PE-conjugated LC3 (LC3–PE) is required for the expansion of autophagic membranes, their ability to recognize autophagic cargoes and the fusion of autophagosomes with lysosomes. The resulting autophagosome fuses with endocytic and lysosomal compartments, ultimately leading to formation of the autolysosome. In microautophagy, substrates are directly engulfed by lysosomal membrane. In chaperone-mediated autophagy (CMA), substrates with the pentapeptide motif KFERQ are selectively recognized by the heat shock cognate 70kDa protein (HSC70) chaperone and translocated to lysosomes in a LAMP2A-dependent manner. In all three processes, the autophagic cargo undergoes the lysosomal degradation (modified figure from [162]).

Autophagosome can engulf bulk cytoplasm non-specifically, including entire organelles, or target cargos specifically. As physiological event, a basal autophagy provides the constitutive turnover and recycling of cytoplasmic components, maintaining cellular homeostasis. During starvation, autophagy is rapidly upregulated to provide an alternative source of energy to maintain essential activity and viability in response to nutrient limitation. Besides this recycling function, autophagy is increasingly recognized as a cellular quality

control mechanism through the removal of damaged or obsolete organelles and proteins, which could become toxic for the cell [152].

3.1.2 Autophagy regulation

Autophagy is highly regulated in order to avoid both insufficient and excessive activation, which may cause inadequate removal of damaged proteins and organelles and thus accumulation of cellular damage or results in cell death respectively. Mammalian autophagosome formation is induced by the activation of the ULK1 complex, which is promoted by suppression of the evolutionarily conserved serine/threonine protein kinase mTOR (mammalian target of rapamycin), the autophagy major regulator. mTOR can be divided into two functionally and biochemically distinct complexes, mTORC1 and mTORC2. Among them, mTORC1 is generally the one associated with cell proliferation and cancer progression when deregulated. mTORC1 is a rapamycin sensitive complex, whose other components are Raptor (regulatory-associated protein of mTOR), GβL/mLST8 (mammalian lethal with Sec13 protein 8), PRAS40 (proline-rich akt substrate 40 kDa), and Deptor (DEP domain-containing mTOR-interacting protein) and exerts a repressor role on the autophagic process. mTORC1 acts as a central regulator of cell growth, proliferation and survival in response to nutritional status, growth factor, and stress signals. In the presence of nutrients, mTORC1 is active and inhibits autophagy by phosphorylating ULK1, as well as ATG13, at multiple residues. Phosphorylation of ULK1 and ATG13 by mTORC1 results in suppression of ULK1 catalytic activity and negatively influences complex translocation to PAS, thus inhibiting autophagy initiation [163]. Upon starvation conditions, mTORC1 is inactivated and both ULK1 and ATG13 are rapidly dephosphorylated, resulting in activation of the ULK1 kinase and concomitant autophagy induction. Indeed, once activated, ULK1 complex translocates to subdomains of the ER where it coordinates the initiation of autophagosomes. Besides the presence of nutrients, mTORC1 can also be regulated by AMP-activated protein kinase (AMPK). AMPK is a key energy sensor, which is activated

in conditions of low ATP levels or increases in the AMP/ATP ratio promoting autophagy. In low energy states, AMPK inactivate mTORC1 through phosphorylation of Raptor, a key protein present within the mTORC1 complex, and through the phosphorylation and activation of the tuberous sclerosis 2 (TSC2) component of the TSC1/2 complex, a negative mTORC1 regulator, leading to the activation of the autophagic pathway. Notably, AMPK can also directly phosphorylate and activate ULK1 at multiple serine residues [164].

Although originally classified as a type of programmed cell death, currently autophagy is more widely viewed as adaptive response to stress conditions acting as a basic cell survival mechanism. In physiological conditions, autophagy have been associated with a wide range of different cellular processes such as the clearance of intracellular microbes during infection, the clearance of ubiquitinated protein aggregates (or inclusion bodies) in neurodegeneration, and tumour suppression [165]. Thus, dysfunctions in the autophagic process results in the onset of a huge variety of pathological conditions [166].

3.2 Autophagy in mesothelioma

The autophagic PI3K/mTOR pathway has been reported to be upregulated in MM. Recently, some researchers have tested the cell growth inhibition properties of two dual PI3K/mTOR inhibitors, NVP-BEZ235 and GDC-0980, on several MM cell lines, identifying resistant and sensitive lines. However, no correlation to the downregulation of PI3K/mTOR activity was found in these conditions. As a result of mTOR inhibition, both drugs efficiently induced long-term autophagy but not cell death. Interestingly, using a classic autophagy inhibitor, chloroquine (CQ), in combination with the dual PI3K/mTOR inhibitors, researchers could block autophagy and significantly induced caspase-independent cell death in MM cell lines [167]. Similarly, another recent study has demonstrated that inhibition of autophagy enhances the pemetrexed and simvastatin-induced apoptosis in a MM cell line. Pemetrexed is a multi-

target antifolate used as the first line treatment for MM (paragraph 1.6). It presents clinical potential, either alone or in combination with *cis-platinum*, and has been shown to inhibit cell proliferation and stimulate apoptosis and autophagy in cancer cells. Simvastatin is a lipophilic drug with anti-cancer effects, mainly through the induction of apoptotic cell death [168]. In this study, researchers have showed that co-treatment with pemetrexed and simvastatin induced greater caspase-dependent apoptosis and autophagy than either drug alone. Interestingly, inhibition of autophagy with 3-methyladenine (3-MA), ATG5 siRNA, bafilomycin A (Baf-A1), and E64D/pepstatin A, enhanced the apoptotic potential of pemetrexed and simvastatin, indicating that pemetrexed and simvastatin-induced autophagy may be a negative regulator of apoptosis [169]. Together, these results suggest that autophagy could be the main mechanism of cell death resistance in MM. To date, however, the molecular mechanisms underlying the interplay between autophagy and apoptosis have not yet been clearly understood.

AIM

Endoplasmic reticulum (ER)-mitochondria calcium (Ca^{2+}) transfer is a key process for Ca^{2+}-dependent cell death signalling. The "quasi-synaptical" feeding of Ca^{2+} to the mitochondria can lead to massive and/or prolonged Ca^{2+} overload into the latter, promoting apoptotic induction. In addition to apoptosis, the ER-mitochondria Ca^{2+} signalling mediated by type III inositol 1,4,5-trisphosphate receptor (IP_3R3) can also modulate autophagy [145]. In response to environmental cues that promote inositol 1,4,5-trisphosphate (IP_3) generation, IP_3Rs, located on the ER, allow Ca^{2+} transfer to mitochondria to promote oxidative phosphorylation. When Ca^{2+} entry into mitochondria decreased, it can result not sufficient for the activation of Kreb's cycle enzymes and the sustainment of the mitochondrial respiration, thus the autophagic process is induced as a survival mechanism to respond to the lack of energy production [146]. In malignant pleural mesothelioma (MPM), a critical dysregulation in Ca^{2+} signalling has been shown to lead to reduced mitochondrial respiration and to an impaired apoptosis. Correction of the intracellular Ca^{2+} signalling resulted in the rescue of efficient apoptotic responses through mitochondrial Ca^{2+}-uptake [144]. By the other hand, the autophagic pathway has been reported to be upregulated in MPM and inhibition of the process with classic autophagy inhibitors, such as chloroquine (CQ) and derivatives, block autophagy and significantly rescue susceptibility to chemo-induced apoptosis in cancer cells [167,169]. Thus, resistance to apoptotic stimuli and chemo-resistance in MPM has been associated to both reduced ER-mitochondria Ca^{2+} transfer [135-137] and autophagy [167,168]. However, it has not been clearly defined whether these two mechanisms are independent each other or are involved in a crosstalk to cooperate in order to exert their pro-survival function in cancer cells. More than 60% of malignant mesotheliomas (MMs) carry mutations in BRCA1-associated protein 1 (BAP1) gene [143]. BAP1 deubiquitylates and stabilizes IP_3R3, allowing Ca^{2+} transfer from the ER to mitochondria promoting apoptosis. Reduced levels of BAP1, in carriers of *BAP1* mutations, cause reduction both of IP_3R3 protein levels and of

ER Ca^{2+} flux to mitochondria, preventing apoptosis and sustaining cell death-resistant in cancer cells [137]. As expected for a gene that has a critical role in cellular physiology, several other genes modulate IP_3R3 activity: *BCL-2* family, *AKT*, *PML*, *PTEN*, *BRCA1*. Moreover *TP53* mutations indirectly influence the same mechanism by reducing ER Ca^{2+} concentrations [145]. Since it is not yet feasible to replace the activity of mutated genes in cancer cells, we hypothesized that by decreasing autophagy we might counteract the deficiency of IP_3R3 induced by mutations of *BAP1* and/or other genes. Resistance to chemotherapy-induced apoptosis is common in MM, and it is probably linked to frequent mutations of *BAP1* (~60%), *TP53* (~10%), and of the other genes that stabilize IP_3R3 [143,22,170]. Recent data suggested that antidepressants (ADs) and antipsychotics (APs) could inhibit autophagy in breast, prostate and bladder cancer cells. Moreover, it has been demonstrated that ADs and APs reduce cancer cell growth synergizing with chemotherapy drugs, such as gemcitabine and mitomycin, in killing cancer cells by blocking autophagy [171]. Here, we investigated the anti-autophagic effects of the ADs, desmethylclomipramine (DCMI) and sertraline, and the APs, clozapine and haloperidol, in primary MM cells derived from patient's biopsies to test whether these drugs would increase the activity of chemotherapy in MM by inducing susceptibility to chemo-induced apoptosis.

RESULTS

1. ADs inhibit the excessive autophagy in cultures obtained from MM patients

We established primary human MM cell cultures from MM patients biopsies; moreover we established cell cultures of primary benign human mesothelial cells (HM, control) from pleural fluids of individuals with non-malignant conditions (Supplemental Figure 1A). We used primary cells, rather than cell lines, to limit the possibility that the results might be influenced by mutations occurring during extensive passage of cells in tissue culture. Cell lines were used to validate the results.

Specific autophagic markers were examined in HM cultures from three different patients, studied between cell culture passages 2-5, and in cultures from five human MM biopsies studied between passages 2-8. The expression levels of the autophagic markers LC3B and p62 were assessed by immunoblotting (Figure 1A). We visualized autophagic vacuoles via live cell microscopy using a GFP-LC3 plasmid (Figure 1B). We found that human MM samples have higher levels of the lipidated form of LC3 (LC3-II) and a reduced amount of p62 protein compared to HM, indicating increased autophagy in MM cells.

To verify that the increased LC3-II levels (Figs 1A-B) were related to increased autophagy in MM cells, rather than to alterations in the autophagic flux, we treated cells with bafilomycin-A1 (Baf-A1), a macrolide that by preventing the passage of protons into the lysosomal lumen disrupts the autophagic flux. When the autophagic flux is disrupted, the amount of the cleaved form of LC3 in resting conditions is similar to that observed after Baf-A1 treatment. In contrast, when the LC3-II levels differ between these two conditions, is evidence that the autophagic flux is maintained [159]. We found that both HM and MM samples have a functional autophagic flux (Figure 1C).

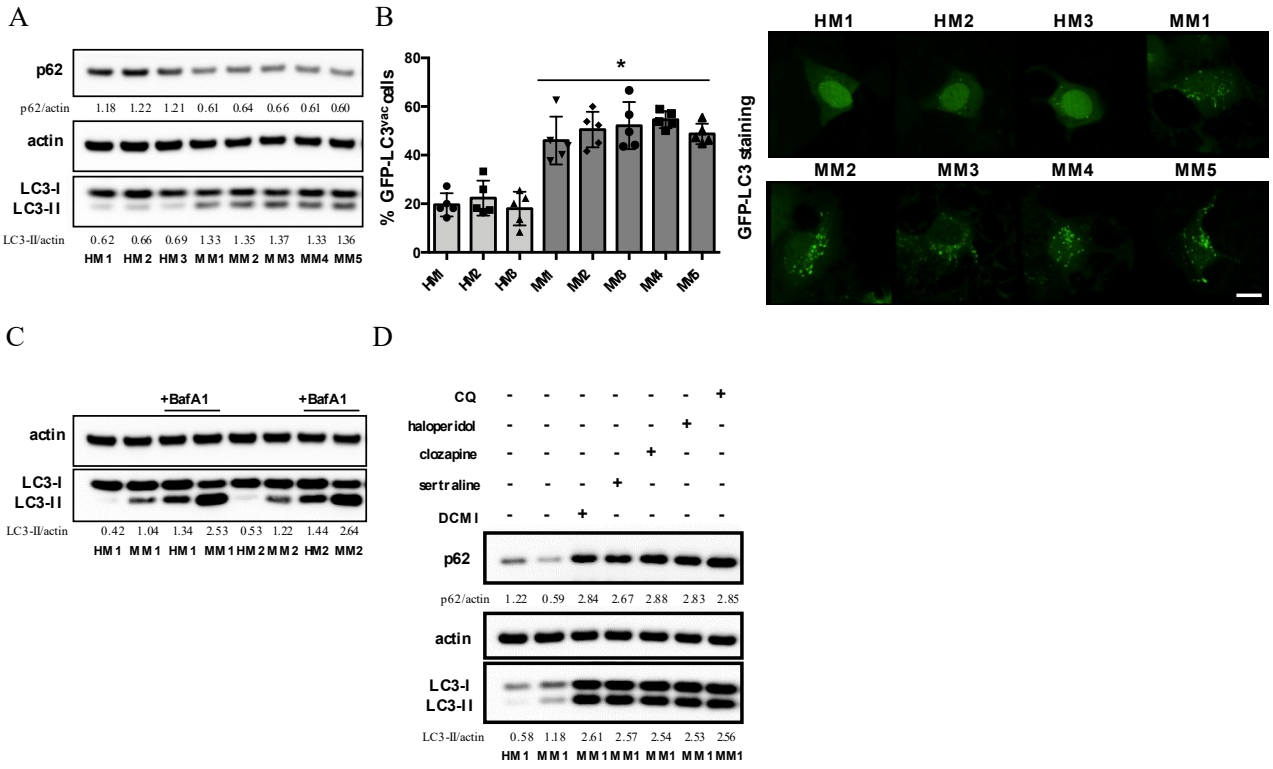

Figure 1. ADs and APs block the excessive autophagy in human MM samples.

(A) Representative immunoblot of the autophagic markers LC3B and p62 in HM and MM samples. **(B)** Cells were infected with an adenovirus carrying the GFP-LC3 plasmid. Autophagic dots were quantified using ImageJ software. The data shown are representative of five independent experiments (mean ± SEM, n=5, P<0.01). Statistical comparisons of groups were performed using ANOVA test. **(C)** Autophagic flux was monitored by quantification of LC3 lipidation following treatment with bafilomycin-A1 (Baf-A1). **(D)**The effects of ADs and APs compounds on the autophagic process were analyzed by an immunoblot assay. The immunoblot is representative of at least three independent experiments.

The increased activation of autophagy in MM cells compared to HM, was further confirmed in MM cell lines (PHI, REN and MPP89) (Supplemental Figure 1, B and C). Because enhanced autophagy supports tumour growth [172], antagonists of autophagy have been used in clinical trials [173]. Recent data suggested that some antidepressants (ADs) and antipsychotics (APs) may possess anti-autophagic effects [171,174,175]. Thus, it has been suggested that these drugs (ADs: DCMI and sertraline; APs: clozapine and haloperidol) interfere with the normal execution of the autophagic flux, similarly to the classical

autophagy inhibitor chloroquine (CQ). We tested the effects of these compounds in primary HM and MM cells. Immunoblot assays showed that ADs and APs promoted the accumulation of both LC3-II and p62, indicating inhibition of the late stages of autophagy (Figure 1D). Thus, ADs and APs inhibit autophagy in MM cells.

2. ADs block autophagy and improve MM cell response to chemotherapy

Since autophagy has been associated to a pro-survival function in MM cells [167,168], we tested whether autophagy inhibition with ADs and APs could increase apoptotic cell death. Neither pemetrexed nor *cis-platinum*, the chemotherapy drugs currently in use against MM, given alone or in combination, induced apoptosis in the MM cultures (Figure 2A and Supplemental Figure 2A-D). In contrast, HM were killed (Figure 2A-C). On the contrary, the ADs, DCMI and sertraline, and the APs, clozapine and haloperidol, sensitized MM cells to apoptosis induced by pemetrexed and Cis-Platinum in MM (Figure 2B-F and Supplemental Figure 2C-G). The ability of ADs and APs to increase chemotherapy-induced apoptosis was observed also in MM cell lines (Supplemental Figure 2E-G). Apoptosis was assessed by measuring two apoptotic markers: cleaved poly (ADP-ribose) polymerase 1 (PARP1) and cleaved Caspase-3 (Cas3) (Figure 2B, D, E, F and Supplemental Figure 2C-G). These results were confirmed using Annexin-V labeling, which allows detection of phosphatidylserine externalization, an early signal of apoptosis (Figure 2C-F). Interestingly, ADs and APs did not cause apoptosis in either HM or MM when used alone (i.e., no Pemetrexed no Cis-Platinum, Figure 2B-F and Supplemental Figure 2C-G).

We performed a genetic ablation of *ATG7* (Supplemental Figure 2H), a gene required for the autophagic process [159]: when *ATG7* was ablated, we increased pemetrexed-induced apoptosis (Supplemental Figure 2I). Furthermore, using classical inhibitors of the early (3-methyladenine, 3-MA) and late (CQ) stages of autophagy we were also able to increase

pemetrexed-induced apoptosis (Supplemental Figure 2J-K). These findings indicate that ADs and APs enhance apoptosis induced by conventional chemotherapy by reducing autophagy.

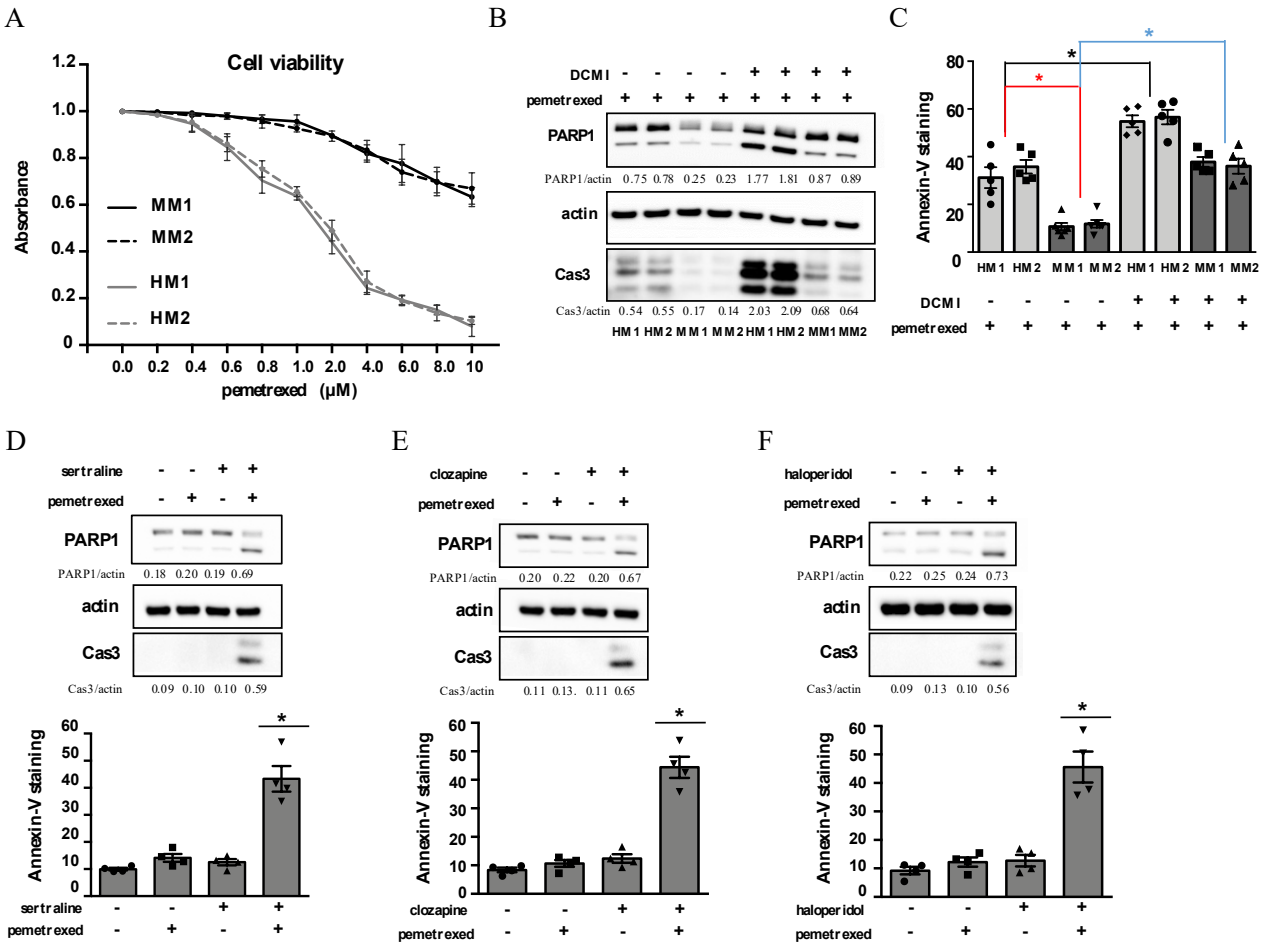

Figure 2. FDA-approved compounds increased the MM cancer cell response to cytotoxic drugs.

(A-C) Human samples obtained from healthy (HM) and MM-affected patients (MM) were treated with pemetrexed alone or in combination with DCMI. The cell viability **(A)** and apoptotic activity **(B-C)** were measured. The graph depicts the Annexin-V intensity expressed as mean ± SEM, n=5, P<0.01. **(D-F)** Similar measurements were carried out in MM samples exposed to treatments combining pemetrexed with sertraline **(D)**, clozapine **(E)** or haloperidol **(F)**. Immunoblots and cell viability plots are representative of three independent experiments. Annexin-V graphs are representative of four independent experiments. Data are expressed as mean ± SEM, n=5, P<0.01 by ANOVA test.

3. ADs modulate apoptosis by regulating ER-mitocondria Ca^{2+} signals

Since ADs and APs modulate autophagy and improve the apoptotic response when given in combination with conventional chemotherapy, we asked whether these drugs exerted this activity via Ca^{2+} signalling. Mitochondrial Ca^{2+} uptake was measured using aequorin technology in response to IP_3-evoked Ca^{2+} stimuli that induce Ca^{2+}-release from the ER via IP_3Rs [176]. Following agonist stimulation, ADs induced a significant increase in Ca^{2+} accumulation in the mitochondrial and cytosolic compartments of MM cells in culture (Figure 3A-B). Similar results were obtained using MM cell lines (Supplemental Figure 3A-B). These findings suggested that ADs restore the Ca^{2+} cross-talk between the ER and mitochondria in MM cells, allowing Ca^{2+}-dependent apoptosis.

This hypothesis was tested via live single-cell imaging with specific Ca^{2+}-sensitive probes to record real-time Ca^{2+} shifts. MM cells were treated with pemetrexed alone or in combination with ADs. Pemetrexed but not ADs induced a modest cytosolic and mitochondrial Ca^{2+} accumulation (Figure 3C-D). However, when cells were pretreated with DCMI and later treated with pemetrexed, we observed major increases in Ca^{2+} concentrations in the cytosol and mitochondria (Figure 3C-D), which caused apoptosis (Figure 2B-C and Supplemental Figure 2C-D). Similar effects were observed in MM cell lines (Supplemental Figure 3C-D).

It has been recently reported that the protein levels of IP_3R3, the main player in Ca^{2+} release from ER, are regulated by ubiquitylation and deubiquitylation [136,137]. Ubiquitylated proteins are degraded by the proteasome; accordingly, the proteasome inhibitor MG132 by blocking the degradative pathway should stabilize IP_3R3 protein levels. MM cells treated with MG132 showed a significant increase in both mitochondrial and cytosolic Ca^{2+} concentrations (Figure 3E-F and Supplemental Figure 3E-F). Accordingly, when MM cells were pretreated

with MG132, the ability of pemetrexed to induce ER Ca^{2+}-release (Figure 3G and Supplemental Figure 3G) and trigger apoptosis was significantly enhanced (Figure 3H).

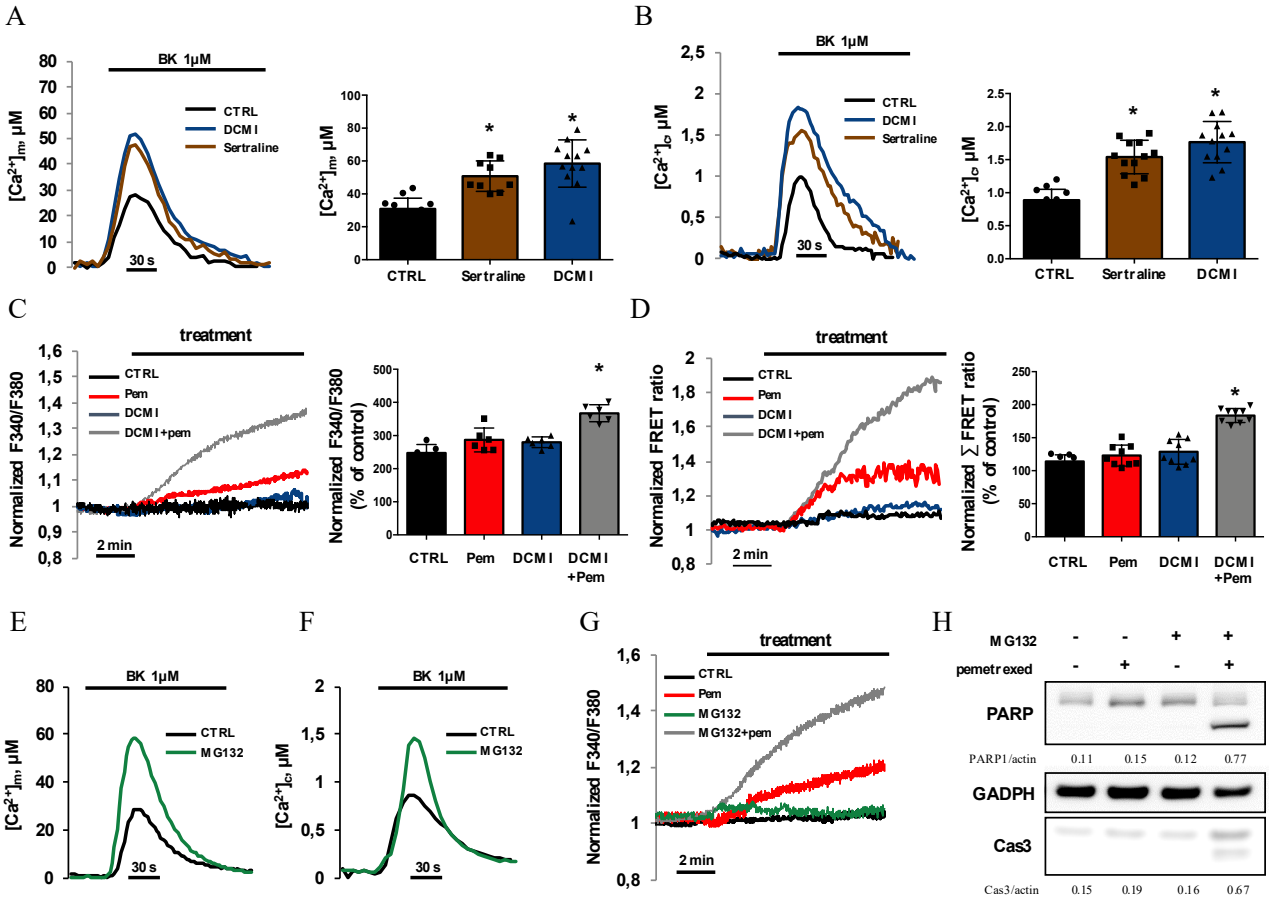

Figure 3. ADs modulate Ca^{2+} transmission between the ER and mitochondria in MM primary cells.

(A-B) Primary MM cells were infected with an adenovirus encoding a mitochondrial **(A)** and cytosolic **(B)** aequorin. To induce the ER-Ca^{2+} release, cells were perfused with bradykinin (BK). Data are shown as mean ± SEM, n = 6–7, **P < 0.01. **(C-D)** ER-Ca^{2+} release was also investigated in live single cells using fluorescence imaging. Primary MM cells were loaded with Ca^{2+} indicator FURA-2 **(C)** or transfecting cells with a plasmid encoding a mitochondrial chameleon **(D)** to measure the cytosolic and mitochondrial Ca^{2+} dynamics, respectively. Data are shown as mean ± SEM, n = 5–7, **P < 0.01. **(E-G)** The aequorin and FURA-2 experiments were replicated upon MG132 treatment. **(H)** The apoptotic potential of MG132 in MM cells was investigated by immunoblot assay (n=3 independent experiments).

4. ADs stabilize IP_3R3 by blocking its degradation

Autophagy and ubiquitin-proteasome system (UPS) are the primary processes involved in cellular degradation and they highly cooperate sharing various pathways and protein partners [151]. In this light, we tested if ADs and inhibitors of UPS could have similar effects in our conditions.

When we treated MM cells with DCMI or MG132, we induced simultaneous increases in the lipidated form of LC3 (LC3-II) and p62 in response to both stimuli (Figure 4A) indicating that the autophagic flux was blocked in both conditions. Moreover, both DCMI and MG132 treatment increased IP_3R3 levels in MM (Figure 4B and Supplemental Figure 4A), and this change was accompanied by a significant increase in protein ubiquitylation (Figure 4C). These same effects were obtained using other ADs (Supplemental Figure 4B), as well as by inhibiting autophagy with genetic ablation of the *ATG7* gene (Supplemental Figure 4C) and by using the classical pharmacological inhibitors CQ and 3-MA (Figures 4D-E and Supplemental Figure 4D).

ADs and MG132-mediated increases in IP_3R3 protein levels were not due to an increased mRNA levels (Supplemental Figure 4E). There were no differences in basal IP_3R3 mRNA levels between MM and HM cells (Supplemental Figure 4F). Instead, we found that both, ADs and MG132 increased the overall amount of protein ubiquitylation in MM cells. Specifically, we observed a significant increase in IP_3R3 ubiquitylation (Figure 4F).

To determine whether this effect was due to an inhibition of proteasome activity, we determined the amount of active proteasomes in living MM cells treated with ADs and MG132 by measuring fluorescence of VF Bodipy, which binds to catalytically active proteasome subunits [177]. A reduction of active proteasomes was observed in cells treated with MG132 and different ADs (Figures 4G-H and supplemental Figures 5A-B). Notably, ADs directly inhibited β1, β2 and β5 active sites of the proteasome semi-purified from MM

cells, as shown by the strong reduction of peptidylglutamyl-peptide hydrolyzing (PGPH), trypsin-like (T-L) and chymotrypsin-like (ChT-L) activities (Figures 4I-K and supplemental Figure 5C).

These findings suggested a possible novel therapeutic approach to sensitize MM cells to chemotherapy-induced apoptosis. However, in spite of significant efforts searching databases and contacting physicians who treat large number of MM patients in the USA and in Europe, we did not find sufficient data to verify whether ADs administration influenced survival of MM patients treated with chemotherapy. The only cohort in which the information about ADs use in MM patients were recorded, were from a small cohort in Lombardia (Italy). These data did not reach significance and lacked valid controls, however they showed a trend suggesting that chemotherapy-treated MM patients who also received ADs may have improved survival (Figure 4L). We specifically, identified 123 MM patients treated with standard first-line chemotherapy, with a mean age of 69.6 ± 7.1 (SD), whose 53 females (43.1%). Among them, there were 13 patients treated with ADs/APs that regulate autophagy; and 12 patients with a reference drug class with no influence on autophagy, angiotensin-converting enzyme (ACE) inhibitors (ACE-I). MM patients treated with ADs/APs showed a tendency towards a lower mortality (HR [CI] 0.60 [0.29-1.24], log-rank test p==0.05) (Figure 4L). Although caution here is appropriate, this encouraging findings may warrant a prospective annotation of the use of ADs and APs in mesothelioma patients undergoing chemotherapy, to see whether the observed improved positive trend in survival is confirmed in a larger cohort.

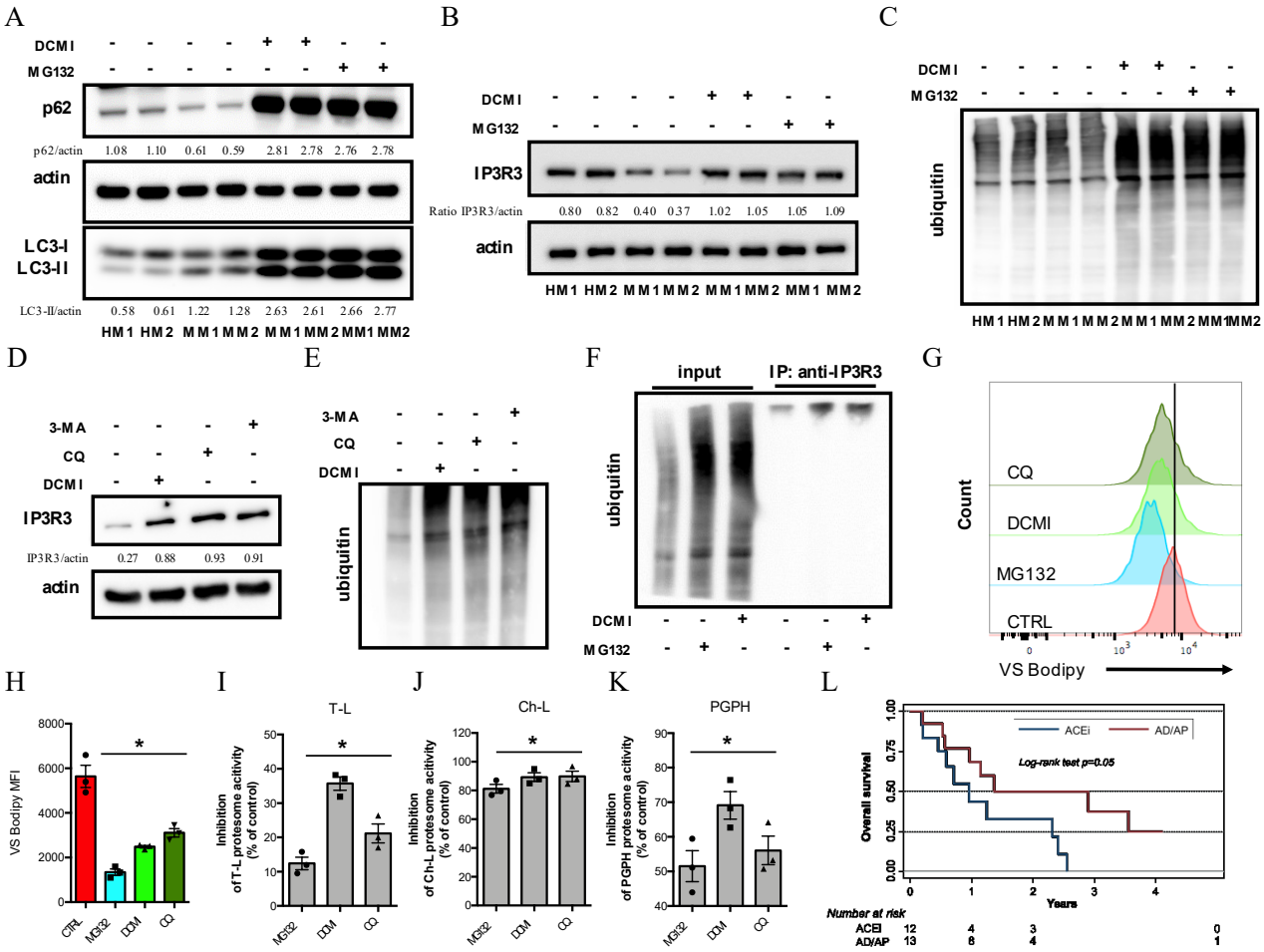

Figure 4. ADs stabilize IP$_3$R3 by blocking degradation events.

(A) MG132 and DCMI exert similar autophagy-blocking effects. **(B-C)** Ability of ADs and the classic UPS inhibitor MG132 to increase the protein accumulation of IP$_3$R3 analyzed via immunoblots **(B)** and by disrupting ubiquitin activities **(C)**. **(D-E)** Similar effects were found after treatment with 3-MA and CQ. **(F)** The selectivity of ADs in modulating the IP$_3$R3 ubiquitination was investigated by immunoprecipitation assays where IP$_3$R3 was used as bait. Immunoblots shown are representative of at least three independent experiments. **(G-H)** Ability of ADs and MG132 to inhibit proteasome activity was measured by flow cytometry. **(I-K)** We obtained same results on semi-purified proteasomes from MM cells. Data are shown as mean ± SEM, n = 3 independent experiments, **P < 0.01. **(L)**The Kaplan-Meier curve compares survival of MM patients from the beginning of the first-line treatment with pemetrexed/Cis-Platinum in the subgroup of patients concomitantly exposed to ADs versus those exposed to ACE-I, drug class with no influence on autophagy.

DISCUSSION

Malignant mesothelioma (MM) is a highly aggressive neoplasm with poor prognosis, which leads to patient death within a few months or years after diagnosis. Presently, no standard curative therapy exists for MM, since this tumour is largely unresponsive to standard chemo- and radio-therapies. Hence, new targets for effective therapeutic strategies are needed and development of novel therapies require a better understanding of the processes that sustain chemo-resistance and that drive MM growth. MM is strongly correlated to exposure to asbestos with a percentage of 90% of positive cases to exposure to this mineral [1]. Nevertheless, there are also rare familial forms of MM, which are linked to germline mutations of several genes (such as BRCA1-associated protein 1, *BAP1*) that can be transmitted from one generation to another [13,15,16]. The presence of a specific genetic background influences the susceptibility to MM, thus representing a risk factor for the development of the malignancy. Mutations of the tumour suppressor BAP1 cause a high incidence of MM [13]. More than 60% of MMs carry mutations in the gene encoding for this protein. Recently, it has been showed that BAP1 localizes at the endoplasmic reticulum (ER), where it binds, deubiquitylates, and stabilizes the type III inositol 1,4,5-trisphosphate receptor (IP_3R3), modulating calcium (Ca^{2+}) release from the ER into the cytosol and mitochondria and promoting apoptosis [137]. In fact, ER-mitochondria Ca^{2+} transfer is a key process for Ca^{2+}-dependent cell death signalling and reduced levels of BAP1, in carriers of *BAP1* mutations, cause reduction both of IP_3R3 protein levels and of ER Ca^{2+} flux to mitochondria, preventing apoptosis and sustaining cell death-resistant in MM cells [137]. In addition, different studies place IP_3R3 in the core of the machinery regulating autophagy [178,179]. Recently, we demonstrated that in cancer cells autophagy is activated when IP_3R3-mediated Ca^{2+} transfer from ER to mitochondria is reduced [147]. Indeed, reduced Ca^{2+} uptake into mitochondria is unable to promote oxidative phosphorylation and to sustain mitochondrial energy production, thus triggering autophagy activation [145]. The autophagic

process is probably induced as a survival mechanism to respond to the lack of energy production [146]. Accordingly, resistance to apoptotic stimuli and chemo-resistance in MM has been associated to both reduced ER-mitochondria Ca^{2+} transfer [135-137] and autophagy [167,168]. Resistance to chemotherapy-induced apoptosis is common in MM, and it is probably linked to frequent mutations of *BAP1* (~60%), *TP53* (~10%), and of the other genes that stabilize IP_3R3 [22,143,170]. Interestingly, independent research groups have shown that MM cell lines have enhanced autophagy levels and that the treatment of MM cells with the classic autophagic inhibitor chloroquine (CQ) improves the anti-proliferative effects of chemotherapy [167,169]. Unfortunately, CQ possesses several undesired side effects and, most important, its exact mechanism of action remains still elusive. So, safer and more efficacious inhibitors could represent a valuable tool for clinic practice. Recent data suggested that antidepressants (ADs) and antipsychotics (APs) could inhibit autophagy in breast, prostate and bladder cancer cells. Moreover, it has been demonstrated that ADs and APs reduce cancer cell growth synergizing with chemotherapy drugs, such as gemcitabine and mitomycin, in killing cancer cells by blocking autophagy [171].

Here, we investigated the anti-autophagic effects of the ADs, desmethylclomipramine (DCMI) and sertraline, and the APs, clozapine and haloperidol, in primary MM cells derived from patient's biopsies. Our data demonstrated that these drugs are effectively autophagic inhibitors (Fig.1D), which improve the efficacy of chemotherapic drugs, pemetrexed and cis-platinum, to promote apoptosis in MM cells (Fig.2B-F and Fig.S2). As reported in Fig.3C-D, we noted that chemotherapic agent pemetrexed alone is unable to activate the Ca^{2+}-transfer from ER to mitochondria necessary to provoke cell death. Whereas, when ADs are added, the amount of mitochondrial Ca^{2+} in a MM cell increases (Fig.3D and Fig.S3) and, therefore, MM cells undergo to apoptosis when exposed to chemotherapy (Fig 2B-F). Thus, we hypothesized that the observed chemo-resistance in MM cells could be due to the reduced IP_3R3 levels compared to healthy mesothelial cells (Fig.4B). Autophagy and the

ubiquitin-proteasome system (UPS) are the two major mechanisms responsible for degradation of cellular components, which functionally cooperate with each other to maintain protein homeostasis. These two pathways share notable similarity in many aspects, in particular during the ubiquitination process [151]. Hence, we asked whether autophagic inhibitors ADs and APs might also modulate the UPS pathway. ADs mediated autophagy inhibition increased IP_3R3 levels in MM cells (Fig.2B and Fig.S4) and this change was accompanied by a significant modification in protein ubiquitylation (Fig.2C). Similar effects were found by using the well-known proteasome inhibitor MG132. In addition, we found a reduction of active proteasomes in living MM cells treated with ADs (Fig.4G-K and Fig.S5). Therefore, these drugs could increase IP_3R3 levels in MM cells by preventing its degradation by the autophagic-UPS system, an effect that leads to increased Ca^{2+} transfer from the ER to mitochondria priming cells for pemetrexed induced apoptosis. Together, these data confirm the idea that autophagy inhibition is helpful to improve the efficacy of chemotherapy. To support their potential usage against MM, we conducted a pharmaco-epidemiological analysis on patients with a diagnosis of MM. We found that MM patients treated with ADs and/or APs showed a tendency towards a lower mortality (Fig.4L), suggesting a possible beneficial effect of ADs and APs in MM patients by increasing their response to conventional chemotherapy.

In conclusion, our results suggest that the chemo-resistance in MM is largely related to reduced levels or activity of the IP_3R3 and consequent lower mitochondrial Ca^{2+} concentrations, which render cancer cells incapable to execute apoptosis. Thus, inhibiting the autophagic-UPS degradation of IP_3R3 in MM cells could stabilize the receptor and it could restore susceptibility to chemo-induced apoptosis. In this light, we propose that ADs and APs, in combination with chemotherapy drugs, could represent a novel therapeutic strategy for MM.

Supplemental Data

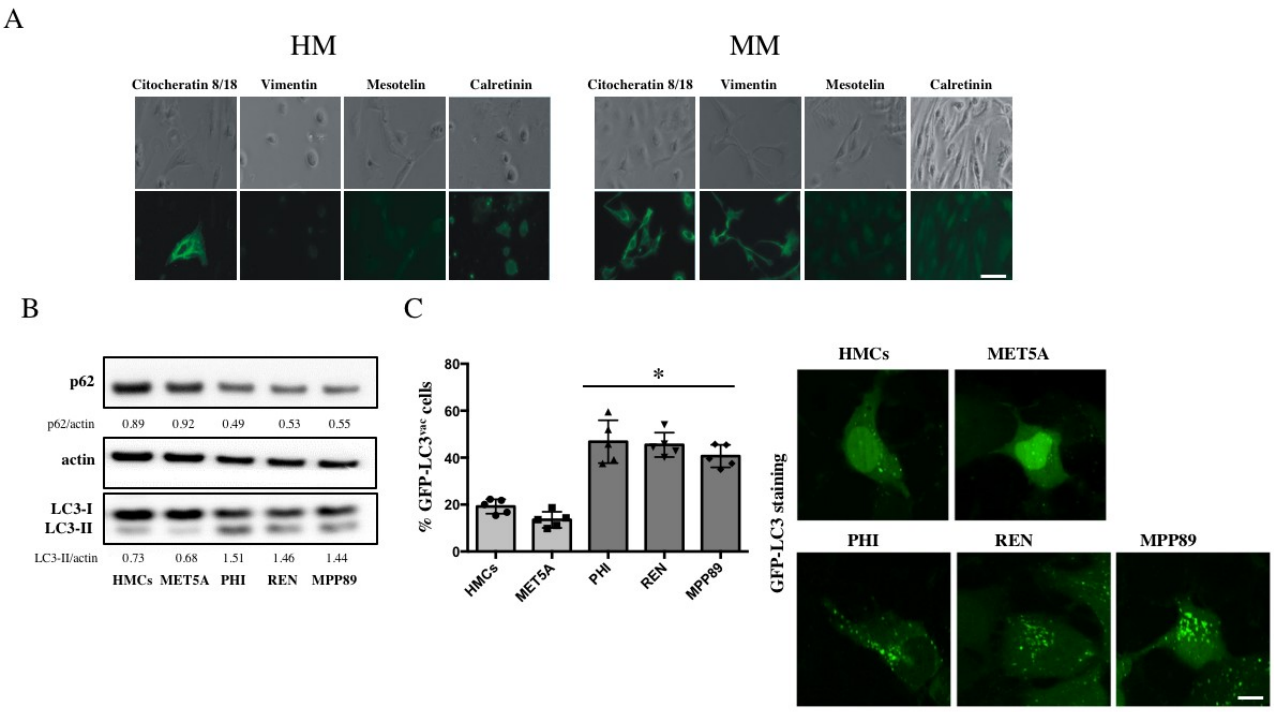

Figure S1. Immortalized mesothelioma cell lines have increased autophagy levels.

(A) Characterization of normal and mesothelioma primary cell samples obtained from healthy and MM-affected individuals. **(B-C)** The autophagic process was analyzed by immunoblotting assay **(B)** and live fluorescence microscopy **(C)** in immortalized mesothelial cells (HMCs and MET5A) and immortalized mesothelioma cell lines (PHI, REN and MPP89). Data are shown as mean ± SEM, n = 5 independent experiments, **P < 0.01, and immunoblot is representative of three independent experiments.

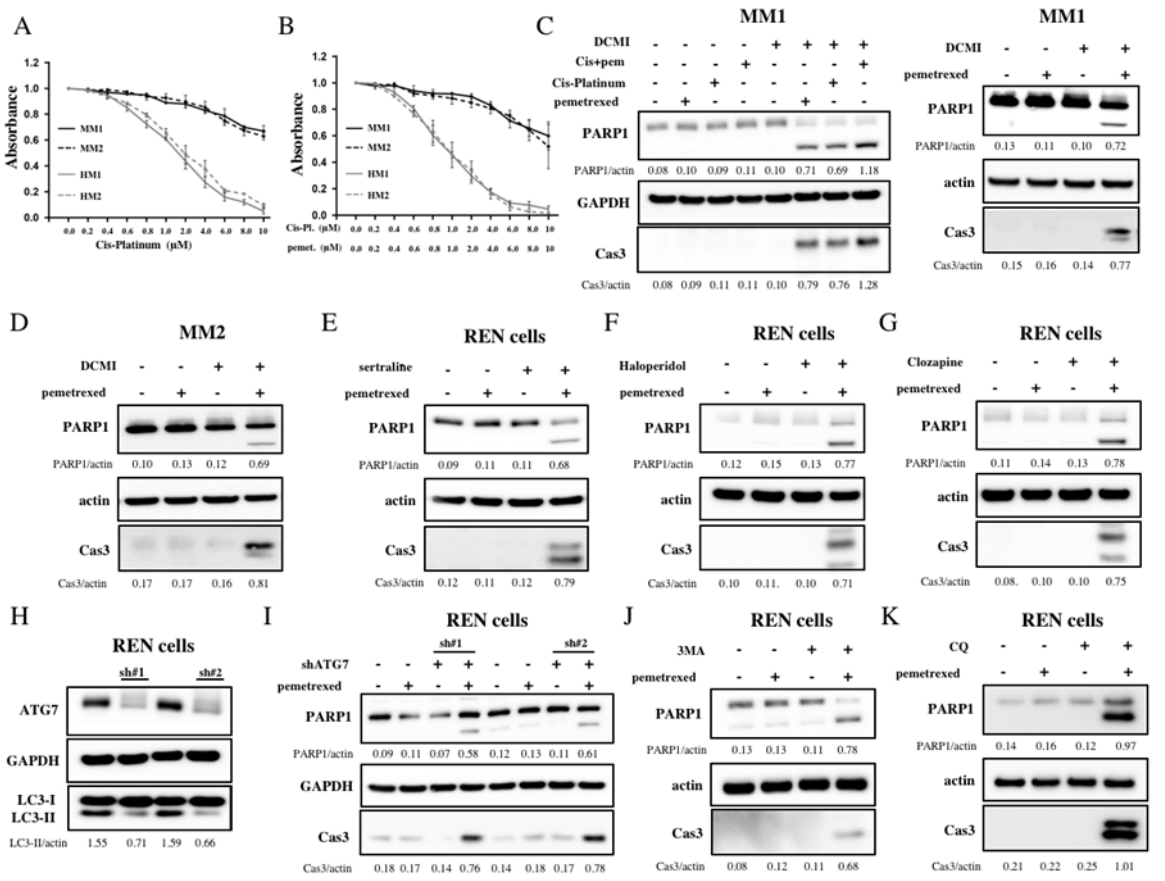

Figure S2. ADs and APs enhance activity of conventional chemotherapy in primary and commercial MM cell lines.

(A-B) Human samples obtained from healthy (HM) and MM-affected patients (MM) were treated with Cis-Platinum alone or in combination with pemetrexed and the cell viability was measured. **(C-D)** Measurement of the apoptotic activity of primary MM cells exposed to pemetrexed and/or Cis-Platinum in combination with DCMI. Combinatory treatment of DCMI and pemetrexed promoted apoptosis in primary human MM cells (MM1 and MM2). Interestingly, single treatment of DCMI did not exert increases in apoptotic levels. **(E-G)** Representative immunoblots showing the efficacy of ADs and APs to improve the apoptotic effect of pemetrexed in a MM cell line. **(H-K)** Similar effects were found after genetic ablation of an essential autophagy gene (ATG7, **H-I**), treatment with an early stage autophagy inhibitor (3-MA, **J**) or a late stage autophagy inhibitor (CQ, **K**). Immunoblots showed are representative of at least three independent experiments.

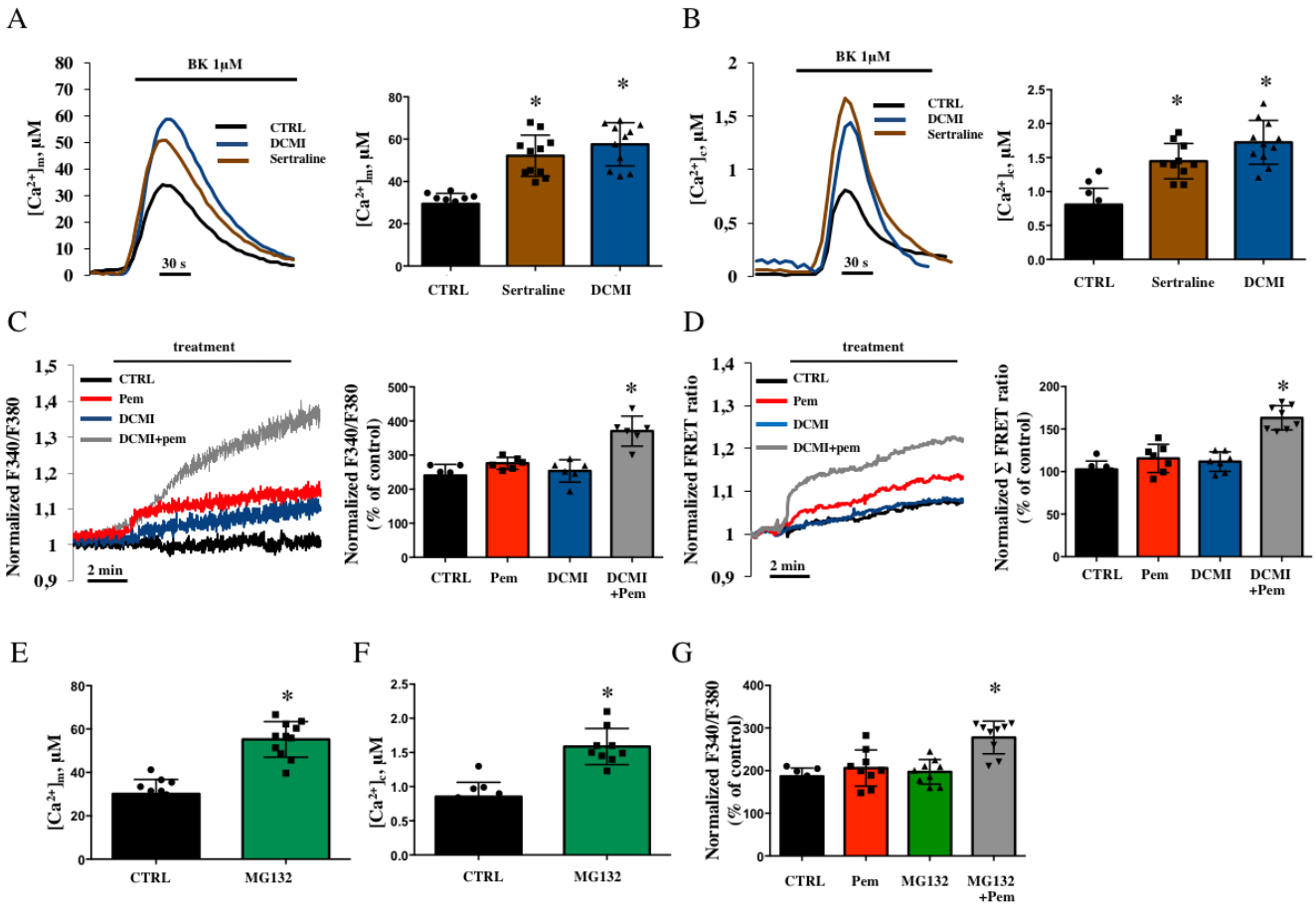

Figure S3. Modulation of Ca^{2+} dynamics in MM cell line exposed to ADs.

(A-B) REN MM cell line was transfected with a mitochondrial **(A)** and cytosolic **(B)** aequorin in order to evaluate the Ca^{2+} accumulation in the mitochondria and in the cytosol. Data are shown as mean ± SEM, n=10, **P < 0.01. **(C-D)** Reactivation of Ca^{2+}-dependent apoptotic events was measured in live single cells using fluorescence imaging. MM cells were loaded with the Ca^{2+} indicator FURA-2 **(C)** or transfected with mitochondrial chameleon **(D)** to measure the cytosolic and mitochondrial Ca^{2+} dynamics, respectively. Data are shown as mean ± SEM, n=7-8, **P < 0.01 **(E-G).** Quantification of the experiments reported in Figure 3E-G. Data are shown as mean ± SEM, n=9-11, **P < 0.01

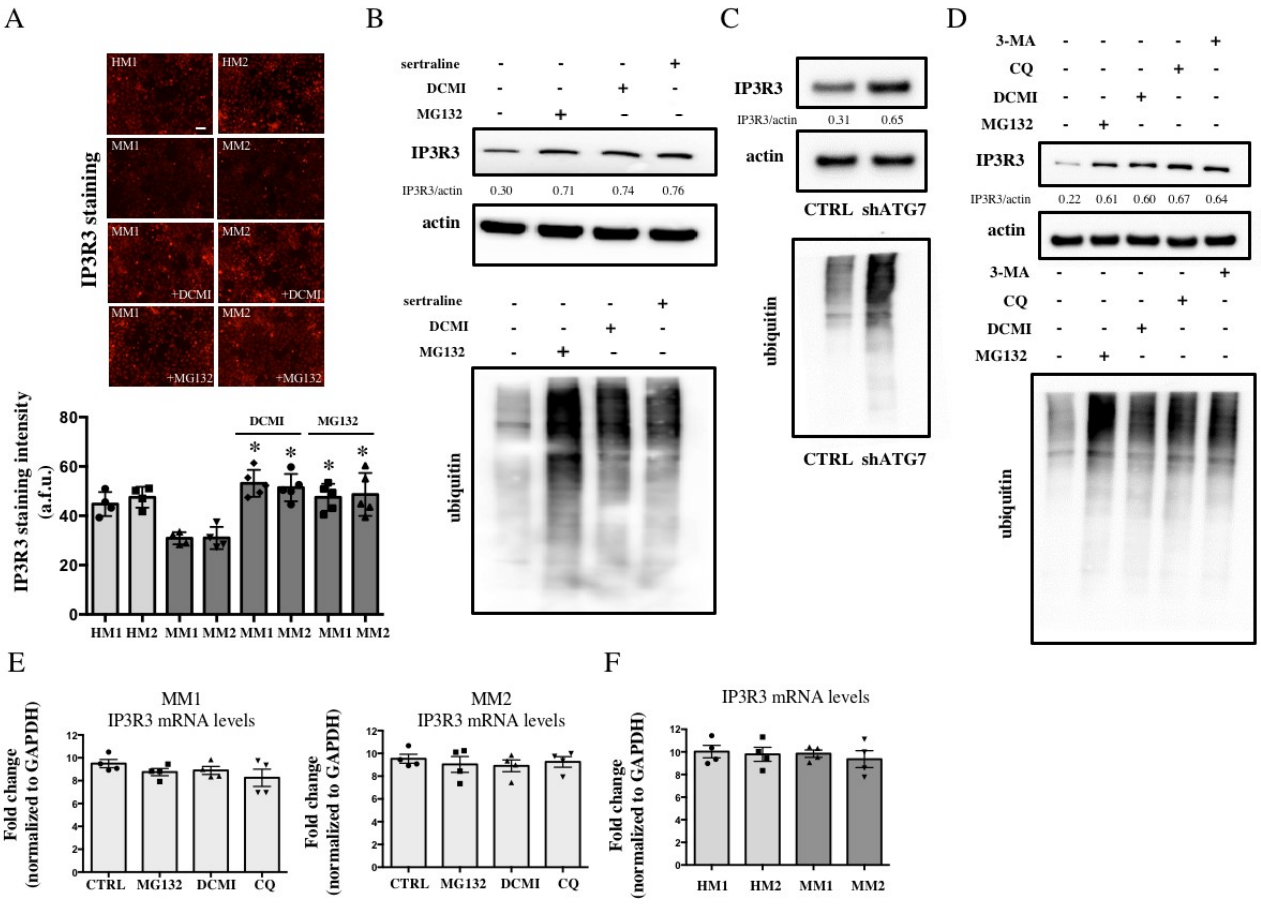

Figure S4. ADs and autophagy inhibitors work on UPS-autophagic process to stabilize IP$_3$R3.

(A) Immunofluorescence staining assay reveals that DCMI and MG132 treatments increase the protein accumulation of IP$_3$R3. The graph represents the mean ± SEM, n=4, **P < 0.01 **(B-D)** The ability of other ADs, MG132 and inhibitors of the autophagic machinery (3-MA, CQ and shATG7) to increase the expression of IP$_3$R3 and modulate ubiquitin activity was evaluated by immunoblotting (n= 3 independent experiments). **(E)** MG132, DCMI and CQ did not modulate the IP$_3$R3 mRNA levels. Data are shown as mean ± SEM, n=4. **(F)** The graph (mean ± SEM, n=4) depicts the IP$_3$R3 mRNA levels in normal and human MM samples.

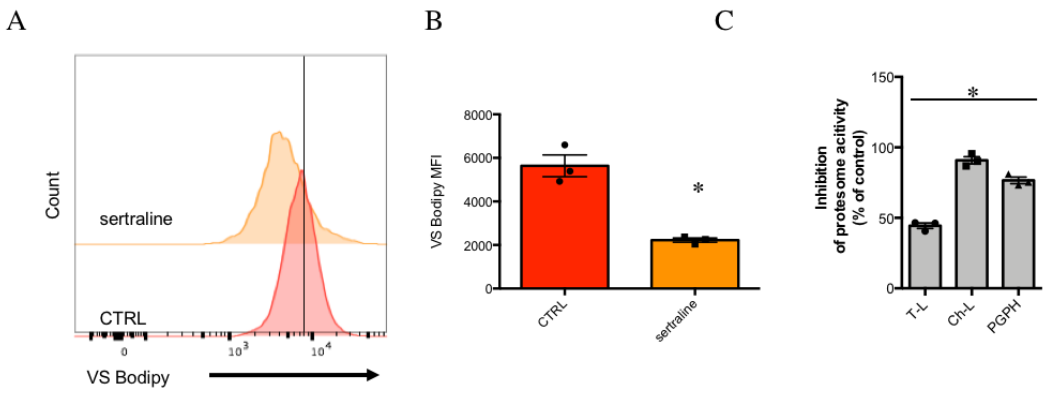

Figure S5. Other ADs inhibit proteasome activity.

The ability of the AD sertraline to inhibit proteasome activity was measured by flow cytometry **(A-B)** and on purified proteasomes from MM cells **(C)**. Data are shown as mean ± SEM, n=3, *P < 0.01

MATERIALS AND METHODS

The study was approved by the Committee for Medical Ethics in Research of the University of Ferrara, and documented informed consent was obtained from participants.

Cell Cultures

Human normal mesothelial cells (HM) and human mesothelioma cells (MM) were obtained from biopsies collected at the Surgical Clinic of the University-Hospital, Ferrara. HM were established from young no oncologic patients (age 29–35 ys) in tissue culture from pleural fluids that accumulated in individuals with congestive heart failure or other non-malignant conditions, who provided previous written informed consent. Primary MM cells were established from tumour biopsies. HM and MM cells were characterized by immunohistochemistry and cultured in Dulbecco's Modified Eagle Medium (DMEM) with 20% fetal bovine serum (FBS) [180-182]. Independent human mesothelial cells cultures from three different donors and independent human mesothelioma cells cultures from five patients were used for the experiments. Each experiment for each of these human mesothelial cell cultures was conducted at least in triplicate. HM cell lines (HMCs and MET5A) and MPM cell lines (REN, PHI and MPP89) were from our cell line collections [144,183].

Growth curves

Cell culture proliferation was measured using crystal violet method. Cells were seeded with a low cell density (10.000 per well) in 6-well plates in triplicate and allowed to grow at 70% of confluence. Cells were then incubated with the indicated compound. After 48h, the cells were washed, fixed with 2% paraformaldehyde and stained with 0.1% crystal violet. After dissolved crystal violet with 1 mol/L acetic acid, the absorbance at 595nm was measured.

Gene silencing with shRNA, adenovirus-mediated gene transfer and transfection

Adenovirus expressing cytosolic aequorin (Ad-cytAEQ), mitochondrial aequorin (Ad-mtAEQ), green fluorescent protein-LC3 (Ad-GFP-LC3) comes from our laboratory [184]. Transfection of mitochondrial-targeted (4mtD3cpv) Ca^{2+} biosensor was performed using Lipofectamine LTX&PLUS (ThermoFisher Scientific). Cells (human mesothelial cells, human mesothelioma cells, HMCs, REN, as indicated in the figures) were seeded and allowed to grow to 60-70% confluence for 36h before transduction or transfection. For aequorin measurements, the cells were seeded onto 13mm glass coverslips. For cell imaging experiments, cells were seeded onto 24mm glass coverslips. For immunoblotting analysis cells were seeded in 6-well plates. For silencing experiments short hairpin RNAs (shRNAs) targeting *ATG7* (sh#1:TRCN 0000151963; sh#2:TRCN 0000151474) were purchased from SigmaAldrich. HEK 293T cells were transfected the indicated shRNAs together with the pVSVG and dr8.2 plasmids in a 3:1:1 ratio using the Lipofectamine 2000 transfection reagent (ThermoFisher Scientific). After 24h, culture medium containing viral particles was collected and passed through 0.8-micron filter. Next, media was added to MM-REN cells with polybrene (10 mg/mL) and incubated at 37°C for 24h. Media was than replenished and cells were selected for puromycin resistance (0.4 mg/mL) for 6 days, after which knockdown was further validated.

Real-Time RT-PCR

1×10^5 cells of HM and MM cells were seeded in 6-well plates. After 36h, total cellular RNA was extracted using an RNeasy Kit (Qiagen, Germany) according to the manufacturer's instructions. Where indicated, before extraction cells were treated with specific compounds as indicated in figures. Extracted RNA was then purified with DNaseI (Takara, Bio Inc. Tokyo, Japan) to remove DNA contamination. 4 μg of total RNA was reverse transcribed into cDNA using the PrimeScriptTM 1st strand cDNA synthesis kit (Takara, Bio Inc. Tokyo,

Japan) according to the manufacturer's instruction. Real-time quantitative analysis of gene expression was performed in a Rotor Gene 2000 Real-Time PCR machine (Qiagen, USA) using the SYBR Green method (AccuPower Green Star qPCR Master Mix; Bioneer, Korea) according to the manufacturer's instructions. Each of the gene expression assays was performed in duplicate and the reaction mixture was composed of 10 μL of SYBR Premix Ex Taq II (Takara, Japan), 10 pmol of each the forward and reverse primers, 2 μL of cDNA, and distilled water to reach a final volume of 20 μL. The thermocycling conditions were performed as follows: one cycle at 95ºC for 10 min, 40 cycles at 95ºC for 20 sec, and 60ºC for 45 sec. Data were normalized with glyceraldehyde-3-phosphate dehydrogenase (GAPDH) as housekeeping gene and endogenous in the same reaction as the gene of interest.

The primers used in this study were as follows:

IP_3R3_RT_F: 5'-TCTTGTTATCAAACTTGTCCCTCTC-3'

IP_3R3_RT_R: 5'-GTCTATGACCTCCTGTTCTTCTTCA-3'

GAPDH_RT_F: 5'-CTTTGTCAAGCTCATTTCCTGG-3'

GAPDH_RT_R: 5'-TCTTCCTCTTGTGCTCTTGC-3'

Aequorin measurements

Experiments were performed by using aequorin technologies as previously described [176]. Cells were incubated with 5 mM coelenterazine (Fluka, 7372) for 2 h in DMEM supplemented with 1% FBS. A 12-mm glass with transfected cells was placed in a perfused thermostated chamber located in close proximity to a low-noise photomultiplier with a built-in amplifier/discriminator. All aequorin experiments were executed in 1 mM Ca^{2+}/KRB supplemented and the agonist was added to the same medium. To determine the remaining aequorin pool, cells were lysed with a hypotonic Ca^{2+}-rich solution (10 mM $CaCl_2$ in H_2O) supplemented of 100 mM digitonin. The luminescence values were determined offline into

[Ca^{2+}] values using a computer algorithm based on the Ca^{2+}-response curve of aequorins. Where indicated, cells were pre-treated with specific compounds.

Intracellular Ca^{2+} measurements

Cells were cultured on 24-mm coverslips and treated with the indicated compounds when cells reached 60% of confluence. Cells were then loaded with the fluorescent Ca^{2+} indicator Fura-2/AM at 37°C for 30min in 1mM Ca^{2+}/Krebs-Ringer buffer supplemented with 0.02% Pluronic F-68 (Merck), 0.1mM sulfinpyrazone (Merck). After three washes, cells were placed on an open Leyden chamber on a 37°C thermostated stage and exposed to 340/380nm wavelength light using the Olympus Xcellence multiple wavelength high-resolution fluorescence microscopy system. Chemotherapic drug was added to the 1mM Ca^{2+}/Krebs-Ringer buffer and the Ca^{2+} release was recorded upon stimulation as indicated in the figures for at least 30 min.

Mitochondrial Ca^{2+} measurements with 4mtD3cpv

Mitochondrial Ca^{2+} dynamics was detected by transfecting cells with the Ca^{2+}-sensitive fluorescence resonance energy transfer (FRET)-based cameleon protein 4mtD3cpv. After 24h, cell were pre-treated with specific compound and imaged with a on a Zeiss Axiovert 200M microscope equipped with C-apochromat 40× oil objective (numerical aperture 1.2) and a cooled CCD camera (Photometrics). The microscope was controlled by MetaFluor 7.0 software (Universal Imaging) and by a Lambda 10-2 filter changer (Sutter Instruments), which permitted to register the emission ratio imaging of the cameleon by using a 436DF20 excitation filter, a 450nm dichroic mirror, and two emission filters (475/40 for enhanced cyan fluorescent protein (ECFP) and 535/25 for citrine). Changes in mitochondrial Ca^{2+} levels were expressed as the ratio of the emissions at 535 and 470 nm. Before analysis, fluorescence images were background corrected.

Co-immunoprecipitation

Mesothelioma cells were treated with the indicated compounds and lysed in buffer containing 30mM Tris-HCl, at pH7.5, 50mM NaCl, 1% NP-40. Extracted proteins pre-cleared by incubating lysates with G-coated Sepharose beads (GE Healthcare) for 1h at 4°C. The supernatant was then collected and quantified. 800 µg (referred to as 'Input') was incubated overnight with IP_3R3 antibody at 4°C. The next day, the precipitation of the immune complexes was performed with G-coated Sepharose beads at 4°C, according to the manufacturer's instructions. After 3h, the beads were washed three times, and finally suspended in 40µL of 2× Laemmli buffer. Ten microliters were loaded on the gel and the samples were processed by SDS– polyacrylamide gel electrophoresis (SDS–PAGE) and analyzed by immunoblot assay.

Antibodies and reagents

For immunoblot and immunostaining analysis, the following antibodies were used: anti-LC3B (Merck, L7543), anti-actin (Merck, A2668), anti-SQSTM1/p62 (Merck, P0067), anti-citokeratin8/18 (abcam, ab17139), anti-calretinin (thermoFisher, MA5-14540) anti-Cas3 (Cell Signaling, 9665), anti-PARP1 (Cell Signaling, 9532), anti-IP_3R3 (BD, 610312), anti-ubiquitin (Cell Signaling, 3933), anti-ATG7 (Cell Signaling, 8558). Other chemicals used are the following: chloroquine (Merck, C6628), haloperidol (Merck, 1303002), clozapine (Merck, 1142107), sertraline (Merck, S6319), Desmethylclomipramine (Merck, N1280), pemetrexed (Merck, 1500659), 3-methyladenine (Merck, M9281), MG132 (Merck, C2211), Bafilomycin A1 (Merck, B1793).

Immunoblotting

Cells were plated in 6-well plates. After 36h, cells were washed three times and collected into ice-cold, phosphate-buffered saline and lysed in a modified 10 mM Tris buffer pH 7.4 containing 150 mM NaCl, 1% Triton X-100, 10% glycerol, 10 mM EDTA and protease

inhibitor cocktail. After 30 min of incubation on ice, homogenates were cleared via centrifugation centrifuged at 12.000 g at 4°C for 10 min. Where indicated, before collection, cells were treated with specific compounds. The supernatatant were collected ant the protein concentrations were determinated by the Lowry procedure. Protein extracts, 15 µg, were separated on 4–12% Bis-Tris acrylamide (Life Technologies, NP0323) and electron-transferred to nitrocellulose membrane according to standard procedures. After saturation of unspecific membranes binding sites with tris-buffered saline (TBS)-Tween 20 (0.05%) supplemented with 5% nonfat powdered milk, membranes were incubated overnight with primary antibodies and the revelation was performed with horseradish peroxidase (HRP)-labeled secondary antibodies [ThermoFisher Scientific, A27036 (goat anti-rabbit) and A28177 (goat anti-mouse)] plus a chemiluminescent substrate (ThermoFisher Scientific, 34080). The chemiluminescence signals were detected using ImageQuant LAS 4010 (GE Healthcare).

Immunofluorescence

Cells previously plated onto 24-mm glasses were washed three times with phosphate buffered saline (PBS), fixed in 2% formaldehyde for 15 min RT and permeabilized for 10 min with 0.1% Triton X-100 in PBS and blocked in PBS containing 2% BSA for 30 min. Cells were then incubated with primary antibody (anti-IP_3R3) overnight at 4°C and washed three times with PBS. The appropriate isotype-matched, AlexaFluor-conjugated secondary antibodies [ThermoFisher Scientific, A-11003 (546 goat anti-mouse)] were used. Images were collected by using a Nikon Swept Field Confocal equipped with CFI Plan Apo VC60XH objective (numerical aperture, 1.4) (Nikon Instruments) and an Andor DU885 electron multiplying chargecoupled device (EM-CCD) camera (Andor Technology Ltd.).

Fluorescence microscopy and quantitative analysis of GFP-LC3 dots

Cells were cultured in a 24 mm glass coverslips and infected at 60% confluence with ad-GFP-LC3. After 36 h, images were taken on a Nikon LiveScan Swept Field Confocal Microscope (SFC) Eclipse Ti equipped with NIS-Elements microscope imaging software (Nikon Instruments). For each condition, the number of GFP-LC3 dots was automatically detected in at least 20 independent visual fields by using ImageJ (Fiji) software.

Quantitative analysis of the autophagic-flux

Primary HM and MM cells were plated in 6-wells. When cells reached 60% confluence, they were treated with the specific inhibitors of lysosomal V-ATPases bafilomycin A1 (BafA1, Sigma) (100 nM) in DMEM with 10% FBS. After 2h, cells were collected for immunoblotting analysis.

Quantitative analysis of proteasome activity

To measure the activity of proteasome of living cells, MM cells were plated in 24-wells. When cells reached 60% confluence, they were treated with the the different compounds for 1 hour and, subsequently, with 2.5 μM VS Bodipy or 2.5 μM S Bodipy for 2 hours at 37°C. VS Bodipy (Me_4BodipyFLAhx$_3$L$_3$VS) and its reduced form (S Bodipy), that constitutes a control probe, are a kind gift of Dr. Salvatore Pacifico (University of Ferrara). Cells were acquired using a BD FACS Canto II (BD Biosciences). Proteasome activity was measured by subtracting S Bodipy mean fluorescent intensity (MFI) from VS Bodipy MFI, after excluding doublets and dead cells by the use of the viability dye Aqua (Life Technologies) as previously described [185].To measure the effects of drugs on specific proteasome subunits, proteasomes were isolated from MM cells as previously described [186]. Suc-LLVY-AMC, Boc-LRR-AMC and Z-LLE-AMC (Sigma) were used to measure ChT-L, T-L and PGPH proteasome activities, respectively. Substrates were incubated at 37 °C for 30 min with proteasomes, untreated or pre-treated with drugs, in activity buffer. Fluorescence was

determined by a fluorimeter (Spectrafluor plus, Tecan, Salzburg, Austria), using an excitation of 360 nm and emission of 465 nm. Activity was evaluated in fluorescence units and the inhibitory activity of the compounds is expressed as compared to untreated (CTRL) proteasomes.

Pharmacoepidemiological analyses

We identified patients with a diagnosis of MM by relevant International Classification of Disease (ICD) 9-CM codes from the Hospital Discharge Forms in a population-based convenience sample of 270.000 subjects from Italy, between 2004 and 2013. Patients who started a first line chemotherapy with cis-platinum (ATC L01XA01) or pemetrexed (ATC L01BA04) were included in the analyses. After record linkage with pharmacy data, concomitant exposure to any of the drugs of interest was defined as at least one drug delivery of antidepressants (ATC N06A) or antipsychotic (ATC N05A) medications, during chemotherapy. ACE-inhibitors (ATC C09A) were chosen as control drug, to limit the bias arising from the association between survival and outpatient drug delivery. This drug class were prescribed in the study sample and has not known anti-autophagy effects. Secondary analysis evaluated the following specific drugs: clomipramine (N06AA04), sertraline (N06AB06), haloperidol (N05AD01) and clozapine (N05AH02). The influence of the concomitant exposure to chemotherapy and antidepressants/anti-psychotics on the overall survival was explored by Kaplan Meier curves and Cox-proportional hazard models by survival analyses and presented as hazard ratio (HR) and 95% confidence intervals (CI).

Statistical analysis

All data presented were analyzed by Prism 6 (GraphPad). Unless otherwise specified in figure legends, data are representative of at least three biologically independent experiments. Two-group datasets were analysed by Student's unpaired t-test. For three or more group analysis, one-way ANOVA with Tukey's multiple comparison test was used.

FUTURE PERSPECTIVES

MM is an aggressive neoplasm of the serosal cavities that exhibits a strong correlation with exposure to asbestos fibers. According to world health organization (WHO) estimates, about 125 million people worldwide are exposed to asbestos at the workplace and at least 107 000 people die each year from asbestos-related diseases, such as mesothelioma [1]. Asbestos indicates a family of minerals, rather common in nature, with a very heat-resistant fibrous structure. The group consists of six naturally occurring mineral silicate fibers of the serpentine and amphibole series, which include the serpentine mineral chrysotile (also known as "white asbestos"), and the five amphibole minerals: actinolite, amosite (also known as "brown asbestos"), anthophyllite, crocidolite (also known as "blue asbestos") and tremolite. The small needle-like fibers that compose the minerals, even more than a thousand times thinner than a human hair, can be inhaled and can damage the mesothelial cells causing several cancers and diseases, including lung cancer, mesothelioma and asbestosis [9,187]. The International Agency for Research on Cancer (IARC) classifies all types of asbestos as carcinogens for humans, although a minor carcinogenic power is described for chrysotile respect to the others [11]. However, little is known about the mechanisms by which asbestos causes the neoplastic transformation of human mesothelial cells. Recently, a primary mechanism has been elucidated. It has been showed that asbestos induces necrotic cell death with resultant release of the protein high-mobility group box 1 (HMGB1) into extra-cellular space and, interestingly, increased serum HMGB1 levels were found in MM patients [188]. Hence, subjects potentially at risk may benefit of an early clinical diagnosis based on HMGB1 as a promising specific biomarker for MM. Notably, HMGB1 functions as a pro-inflammatory cytokine and is one of the most intriguing molecules in inflammatory disorders and cancers. Despite that, HMGB1 is an abundant nonhistone protein that play a central role in the induction of autophagy and it has been reported to be a key regulator of the transcriptional alterations induced by asbestos [189]. In this light, since our results and other

evidences suggest that autophagy is an indispensable component during the chemo-resistance and the progression of MM, we asked whether HMGB1-induced autophagy could be involved in the neoplastic transformation of mesothelial cells caused by asbestos. Thus, we started to investigate the effects of the exposure to different asbestos fibers in primary cells isolated from healthy human mesothelium (HM cells). Our preliminary data report that the fibers prompt different intracellular cell death pathways in HM cells by inducing mitochondrial reactive oxygen species (ROS) production. Interestingly, also the autophagic machinery is highly activated and HMGB1 translocation, from nucleus to cytosol, seems to be fundamental to induce the process. Therefore, we asked whether HMGB1 silencing could prevent the increase of autophagy in HM cells exposed to asbestos, leading to an increase of cell death. Our preliminary data seem to confirm this hypothesis, indicating that HMGB1-mediated autophagy could sustain the tumoral transformation of HM cells caused by asbestos fibers. In summary, our preliminary data suggest that mitochondrial ROS production could be induced in HM cells, after exposure to asbestos, as stress signal that, through the translocation of HMGB1, from the nucleus to the cytoplasm, activate the autophagic process promoting cell death resistance and supporting tumoral transformation. However, research on the role of autophagy in MM and other cancer diseases is still in its infancy and many questions remain concerning the precise mechanisms by which autophagy is involved in carcinogenesis and tumour progression.

REFERENCES

1 Mutti, L. *et al.* Scientific Advances and New Frontiers in Mesothelioma Therapeutics. *Journal of thoracic oncology : official publication of the International Association for the Study of Lung Cancer* **13**, 1269-1283, doi:10.1016/j.jtho.2018.06.011 (2018).

2 Ismail-Khan, R. *et al.* Malignant pleural mesothelioma: a comprehensive review. *Cancer control : journal of the Moffitt Cancer Center* **13**, 255-263, doi:10.1177/107327480601300402 (2006).

3 Segura-Gonzalez, M., Urias-Rocha, J. & Castelan-Pedraza, J. Malignant Mesothelioma of the Tunica Vaginalis: A Rare Neoplasm--Case Report and Literature Review. *Clinical genitourinary cancer* **13**, e401-405, doi:10.1016/j.clgc.2015.05.009 (2015).

4 Magnani, C. *et al.* Pleural mesothelioma: epidemiological and public health issues. Report from the Second Italian Consensus Conference on Pleural Mesothelioma. *La Medicina del lavoro* **104**, 191-202 (2013).

5 Nicholson, W. J., Perkel, G. & Selikoff, I. J. Occupational exposure to asbestos: population at risk and projected mortality--1980-2030. *American journal of industrial medicine* **3**, 259-311, doi:10.1002/ajim.4700030305 (1982).

6 Crocetti, E. & Group, A. W. [Italy. The seven tumors with the worst prognosis]. *Epidemiologia e prevenzione* **33**, 64 (2009).

7 Marinaccio, A., Nesti, M. & Regional Operational, C. Analysis of survival of mesothelioma cases in the Italian register (ReNaM). *European journal of cancer* **39**, 1290-1295, doi:10.1016/s0959-8049(03)00233-8 (2003).

8 Baumann, F., Ambrosi, J. P. & Carbone, M. Asbestos is not just asbestos: an unrecognised health hazard. *The Lancet. Oncology* **14**, 576-578, doi:10.1016/S1470-2045(13)70257-2 (2013).

9 Doll, R. Mortality from lung cancer in asbestos workers. *British journal of industrial medicine* **12**, 81-86, doi:10.1136/oem.12.2.81 (1955).

10 Magnani, C. *et al.* Cancer risk after cessation of asbestos exposure: a cohort study of Italian asbestos cement workers. *Occupational and environmental medicine* **65**, 164-170, doi:10.1136/oem.2007.032847 (2008).

11 Humans, I. W. G. o. t. E. o. C. R. t. Arsenic, metals, fibres, and dusts. *IARC monographs on the evaluation of carcinogenic risks to humans* **100**, 11-465 (2012).

12 Metintas, S., Ak, G. & Metintas, M. A review of the cohorts with environmental and occupational mineral fiber exposure. *Archives of environmental & occupational health* **74**, 76-84, doi:10.1080/19338244.2018.1467873 (2019).

13 Testa, J. R. *et al.* Germline BAP1 mutations predispose to malignant mesothelioma. *Nature genetics* **43**, 1022-1025, doi:10.1038/ng.912 (2011).

14 Ascoli, V. *et al.* Familial malignant mesothelioma: a population-based study in central Italy (1980-2012). *Cancer epidemiology* **38**, 273-278, doi:10.1016/j.canep.2014.02.014 (2014).

15 Xu, J. *et al.* Germline mutation of Bap1 accelerates development of asbestos-induced malignant mesothelioma. *Cancer research* **74**, 4388-4397, doi:10.1158/0008-5472.CAN-14-1328 (2014).

16 Pastorino, S. *et al.* A Subset of Mesotheliomas With Improved Survival Occurring in Carriers of BAP1 and Other Germline Mutations. *Journal of clinical oncology : official journal of the*

American Society of Clinical Oncology, JCO2018790352, doi:10.1200/JCO.2018.79.0352 (2018).

17 Sekido, Y. Molecular pathogenesis of malignant mesothelioma. *Carcinogenesis* **34**, 1413-1419, doi:10.1093/carcin/bgt166 (2013).

18 Carbone, M. *et al.* BAP1 and cancer. *Nature reviews. Cancer* **13**, 153-159, doi:10.1038/nrc3459 (2013).

19 Neri, M. *et al.* Genetic susceptibility to malignant pleural mesothelioma and other asbestos-associated diseases. *Mutation research* **659**, 126-136, doi:10.1016/j.mrrev.2008.02.002 (2008).

20 Shukuya, T. *et al.* Identification of actionable mutations in malignant pleural mesothelioma. *Lung cancer* **86**, 35-40, doi:10.1016/j.lungcan.2014.08.004 (2014).

21 Cadby, G. *et al.* A genome-wide association study for malignant mesothelioma risk. *Lung cancer* **82**, 1-8, doi:10.1016/j.lungcan.2013.04.018 (2013).

22 Bueno, R. *et al.* Comprehensive genomic analysis of malignant pleural mesothelioma identifies recurrent mutations, gene fusions and splicing alterations. *Nature genetics* **48**, 407-416, doi:10.1038/ng.3520 (2016).

23 Gordon, G. J. *et al.* Inhibitor of apoptosis proteins are regulated by tumour necrosis factor-alpha in malignant pleural mesothelioma. *The Journal of pathology* **211**, 439-446, doi:10.1002/path.2120 (2007).

24 Goodman, J. E., Nascarella, M. A. & Valberg, P. A. Ionizing radiation: a risk factor for mesothelioma. *Cancer causes & control : CCC* **20**, 1237-1254, doi:10.1007/s10552-009-9357-4 (2009).

25 Carbone, M. Simian virus 40 and human tumors: It is time to study mechanisms. *Journal of cellular biochemistry* **76**, 189-193, doi:10.1002/(sici)1097-4644(20000201)76:2<189::aid-jcb3>3.0.co;2-j (1999).

26 Carbone, M., Rizzo, P. & Pass, H. Simian virus 40: the link with human malignant mesothelioma is well established. *Anticancer research* **20**, 875-877 (2000).

27 Gazdar, A. F. & Carbone, M. Molecular pathogenesis of malignant mesothelioma and its relationship to simian virus 40. *Clinical lung cancer* **5**, 177-181, doi:10.3816/CLC.2003.n.031 (2003).

28 Vogelzang, N. J. *et al.* Phase III study of pemetrexed in combination with cisplatin versus cisplatin alone in patients with malignant pleural mesothelioma. *Journal of clinical oncology : official journal of the American Society of Clinical Oncology* **21**, 2636-2644, doi:10.1200/JCO.2003.11.136 (2003).

29 McCambridge, A. J. *et al.* Progress in the Management of Malignant Pleural Mesothelioma in 2017. *Journal of thoracic oncology : official publication of the International Association for the Study of Lung Cancer* **13**, 606-623, doi:10.1016/j.jtho.2018.02.021 (2018).

30 Zalcman, G. *et al.* Bevacizumab for newly diagnosed pleural mesothelioma in the Mesothelioma Avastin Cisplatin Pemetrexed Study (MAPS): a randomised, controlled, open-label, phase 3 trial. *Lancet* **387**, 1405-1414, doi:10.1016/S0140-6736(15)01238-6 (2016).

31 Scherpereel, A., Wallyn, F., Albelda, S. M. & Munck, C. Novel therapies for malignant pleural mesothelioma. *The Lancet. Oncology* **19**, e161-e172, doi:10.1016/S1470-2045(18)30100-1 (2018).

32 Berridge, M. J., Lipp, P. & Bootman, M. D. The versatility and universality of calcium signalling. *Nature reviews. Molecular cell biology* **1**, 11-21, doi:10.1038/35036035 (2000).

33 Rizzuto, R. & Pozzan, T. Microdomains of intracellular Ca2+: molecular determinants and functional consequences. *Physiological reviews* **86**, 369-408, doi:10.1152/physrev.00004.2005 (2006).

34 Brini, M. & Carafoli, E. Calcium pumps in health and disease. *Physiological reviews* **89**, 1341-1378, doi:10.1152/physrev.00032.2008 (2009).

35 Carafoli, E. The plasma membrane calcium pump in the hearing process: physiology and pathology. *Science China. Life sciences* **54**, 686-690, doi:10.1007/s11427-011-4200-z (2011).

36 Morgan, A. J. & Thomas, A. P. Single-cell and subcellular measurement of intracellular Ca(2)+ concentration. *Methods in molecular biology* **312**, 87-117, doi:10.1385/1-59259-949-4:087 (2005).

37 Jaffe, L. On the conservation of fast calcium wave speeds. *Cell calcium* **32**, 217-229, doi:10.1016/s0143416002001574 (2002).

38 Petersen, O. H., Burdakov, D. & Tepikin, A. V. Regulation of store-operated calcium entry: lessons from a polarized cell. *European journal of cell biology* **78**, 221-223, doi:10.1016/s0171-9335(99)80054-5 (1999).

39 Guerini, D., Garcia-Martin, E., Zecca, A., Guidi, F. & Carafoli, E. The calcium pump of the plasma membrane: membrane targeting, calcium binding sites, tissue-specific isoform expression. *Acta physiologica Scandinavica. Supplementum* **643**, 265-273 (1998).

40 Blaustein, M. P. & Lederer, W. J. Sodium/calcium exchange: its physiological implications. *Physiological reviews* **79**, 763-854, doi:10.1152/physrev.1999.79.3.763 (1999).

41 Lacinova, L. Voltage-dependent calcium channels. *General physiology and biophysics* **24 Suppl 1**, 1-78 (2005).

42 McFadzean, I. & Gibson, A. The developing relationship between receptor-operated and store-operated calcium channels in smooth muscle. *British journal of pharmacology* **135**, 1-13, doi:10.1038/sj.bjp.0704468 (2002).

43 Meldolesi, J. & Pozzan, T. Pathways of Ca2+ influx at the plasma membrane: voltage-, receptor-, and second messenger-operated channels. *Experimental cell research* **171**, 271-283, doi:10.1016/0014-4827(87)90161-3 (1987).

44 Bezprozvanny, I. The inositol 1,4,5-trisphosphate receptors. *Cell calcium* **38**, 261-272, doi:10.1016/j.ceca.2005.06.030 (2005).

45 Patterson, R. L., Boehning, D. & Snyder, S. H. Inositol 1,4,5-trisphosphate receptors as signal integrators. *Annual review of biochemistry* **73**, 437-465, doi:10.1146/annurev.biochem.73.071403.161303 (2004).

46 Fill, M. & Copello, J. A. Ryanodine receptor calcium release channels. *Physiological reviews* **82**, 893-922, doi:10.1152/physrev.00013.2002 (2002).

47 Berridge, M. J. Inositol trisphosphate and calcium signalling. *Nature* **361**, 315-325, doi:10.1038/361315a0 (1993).

48 Lisek, M., Boczek, T. & Zylinska, L. Calcium as a Trojan horse in mental diseases-The role of PMCA and PMCA-interacting proteins in bipolar disorder and schizophrenia. *Neuroscience letters* **663**, 48-54, doi:10.1016/j.neulet.2017.08.005 (2018).

49 Lytton, J. Na+/Ca2+ exchangers: three mammalian gene families control Ca2+ transport. *The Biochemical journal* **406**, 365-382, doi:10.1042/BJ20070619 (2007).

50 Groenendyk, J., Lynch, J. & Michalak, M. Calreticulin, Ca2+, and calcineurin - signaling from the endoplasmic reticulum. *Molecules and cells* **17**, 383-389 (2004).

51 Michalak, M., Mariani, P. & Opas, M. Calreticulin, a multifunctional Ca2+ binding chaperone of the endoplasmic reticulum. *Biochemistry and cell biology = Biochimie et biologie cellulaire* **76**, 779-785, doi:10.1139/bcb-76-5-779 (1998).

52 John, L. M., Lechleiter, J. D. & Camacho, P. Differential modulation of SERCA2 isoforms by calreticulin. *The Journal of cell biology* **142**, 963-973, doi:10.1083/jcb.142.4.963 (1998).

53 Rizzuto, R. *et al.* Ca(2+) transfer from the ER to mitochondria: when, how and why. *Biochimica et biophysica acta* **1787**, 1342-1351, doi:10.1016/j.bbabio.2009.03.015 (2009).

54 Pinton, P., Pozzan, T. & Rizzuto, R. The Golgi apparatus is an inositol 1,4,5-trisphosphate-sensitive Ca2+ store, with functional properties distinct from those of the endoplasmic reticulum. *The EMBO journal* **17**, 5298-5308, doi:10.1093/emboj/17.18.5298 (1998).

55 Takeuchi, A., Kim, B. & Matsuoka, S. The destiny of Ca(2+) released by mitochondria. *The journal of physiological sciences : JPS* **65**, 11-24, doi:10.1007/s12576-014-0326-7 (2015).

56 Rodriguez, A., Webster, P., Ortego, J. & Andrews, N. W. Lysosomes behave as Ca2+-regulated exocytic vesicles in fibroblasts and epithelial cells. *The Journal of cell biology* **137**, 93-104, doi:10.1083/jcb.137.1.93 (1997).

57 Lasorsa, F. M. *et al.* Peroxisomes as novel players in cell calcium homeostasis. *The Journal of biological chemistry* **283**, 15300-15308, doi:10.1074/jbc.M800648200 (2008).

58 Bootman, M. D., Petersen, O. H. & Verkhratsky, A. The endoplasmic reticulum is a focal point for co-ordination of cellular activity. *Cell calcium* **32**, 231-234, doi:10.1016/s0143416002002002 (2002).

59 MacKrill, J. J. Protein-protein interactions in intracellular Ca2+-release channel function. *The Biochemical journal* **337 (Pt 3)**, 345-361 (1999).

60 Foskett, J. K., White, C., Cheung, K. H. & Mak, D. O. Inositol trisphosphate receptor Ca2+ release channels. *Physiological reviews* **87**, 593-658, doi:10.1152/physrev.00035.2006 (2007).

61 Nakamura, Y. & Fukami, K. Regulation and physiological functions of mammalian phospholipase C. *Journal of biochemistry* **161**, 315-321, doi:10.1093/jb/mvw094 (2017).

62 Litjens, T. *et al.* Phospholipase C-gamma1 is required for the activation of store-operated Ca2+ channels in liver cells. *The Biochemical journal* **405**, 269-276, doi:10.1042/BJ20061762 (2007).

63 Nucifora, F. C., Jr., Li, S. H., Danoff, S., Ullrich, A. & Ross, C. A. Molecular cloning of a cDNA for the human inositol 1,4,5-trisphosphate receptor type 1, and the identification of a third alternatively spliced variant. *Brain research. Molecular brain research* **32**, 291-296, doi:10.1016/0169-328x(95)00089-b (1995).

64 Iwai, M. *et al.* Molecular cloning of mouse type 2 and type 3 inositol 1,4,5-trisphosphate receptors and identification of a novel type 2 receptor splice variant. *The Journal of biological chemistry* **280**, 10305-10317, doi:10.1074/jbc.M413824200 (2005).

65 Taylor, C. W., Genazzani, A. A. & Morris, S. A. Expression of inositol trisphosphate receptors. *Cell calcium* **26**, 237-251, doi:10.1054/ceca.1999.0090 (1999).

66 Iwai, M., Michikawa, T., Bosanac, I., Ikura, M. & Mikoshiba, K. Molecular basis of the isoform-specific ligand-binding affinity of inositol 1,4,5-trisphosphate receptors. *The Journal of biological chemistry* **282**, 12755-12764, doi:10.1074/jbc.M609833200 (2007).

67 Supattapone, S., Worley, P. F., Baraban, J. M. & Snyder, S. H. Solubilization, purification, and characterization of an inositol trisphosphate receptor. *The Journal of biological chemistry* **263**, 1530-1534 (1988).

68 Mignery, G. A., Newton, C. L., Archer, B. T., 3rd & Sudhof, T. C. Structure and expression of the rat inositol 1,4,5-trisphosphate receptor. *The Journal of biological chemistry* **265**, 12679-12685 (1990).

69 Yoshikawa, F. *et al.* Mutational analysis of the ligand binding site of the inositol 1,4,5-trisphosphate receptor. *The Journal of biological chemistry* **271**, 18277-18284, doi:10.1074/jbc.271.30.18277 (1996).

70 Chan, J. *et al.* Structural studies of inositol 1,4,5-trisphosphate receptor: coupling ligand binding to channel gating. *The Journal of biological chemistry* **285**, 36092-36099, doi:10.1074/jbc.M110.140160 (2010).

71 Sienaert, I. *et al.* Localization and function of a calmodulin-apocalmodulin-binding domain in the N-terminal part of the type 1 inositol 1,4,5-trisphosphate receptor. *The Biochemical journal* **365**, 269-277, doi:10.1042/BJ20020144 (2002).

72 Khan, M. T., Wagner, L., 2nd, Yule, D. I., Bhanumathy, C. & Joseph, S. K. Akt kinase phosphorylation of inositol 1,4,5-trisphosphate receptors. *The Journal of biological chemistry* **281**, 3731-3737, doi:10.1074/jbc.M509262200 (2006).

73 Straub, S. V., Wagner, L. E., 2nd, Bruce, J. I. & Yule, D. I. Modulation of cytosolic calcium signaling by protein kinase A-mediated phosphorylation of inositol 1,4,5-trisphosphate receptors. *Biological research* **37**, 593-602, doi:10.4067/s0716-97602004000400013 (2004).

74 Colbran, R. J. Targeting of calcium/calmodulin-dependent protein kinase II. *The Biochemical journal* **378**, 1-16, doi:10.1042/BJ20031547 (2004).

75 Vermassen, E. *et al.* Regulation of the phosphorylation of the inositol 1,4,5-trisphosphate receptor by protein kinase C. *Biochemical and biophysical research communications* **319**, 888-893, doi:10.1016/j.bbrc.2004.05.071 (2004).

76 Murthy, K. S. & Zhou, H. Selective phosphorylation of the IP3R-I in vivo by cGMP-dependent protein kinase in smooth muscle. *American journal of physiology. Gastrointestinal and liver physiology* **284**, G221-230, doi:10.1152/ajpgi.00401.2002 (2003).

77 Jayaraman, T., Ondrias, K., Ondriasova, E. & Marks, A. R. Regulation of the inositol 1,4,5-trisphosphate receptor by tyrosine phosphorylation. *Science* **272**, 1492-1494, doi:10.1126/science.272.5267.1492 (1996).

78 Vanderheyden, V. *et al.* Regulation of inositol 1,4,5-trisphosphate-induced Ca2+ release by reversible phosphorylation and dephosphorylation. *Biochimica et biophysica acta* **1793**, 959-970, doi:10.1016/j.bbamcr.2008.12.003 (2009).

79 Sayers, L. G. *et al.* Intracellular targeting and homotetramer formation of a truncated inositol 1,4,5-trisphosphate receptor-green fluorescent protein chimera in Xenopus laevis oocytes: evidence for the involvement of the transmembrane spanning domain in endoplasmic reticulum targeting and homotetramer complex formation. *The Biochemical journal* **323 (Pt 1)**, 273-280, doi:10.1042/bj3230273 (1997).

80 Mignery, G. A. & Sudhof, T. C. The ligand binding site and transduction mechanism in the inositol-1,4,5-triphosphate receptor. *The EMBO journal* **9**, 3893-3898 (1990).

81 Parker, I., Choi, J. & Yao, Y. Elementary events of InsP3-induced Ca2+ liberation in Xenopus oocytes: hot spots, puffs and blips. *Cell calcium* **20**, 105-121, doi:10.1016/s0143-4160(96)90100-1 (1996).

82 Allbritton, N. L. & Meyer, T. Localized calcium spikes and propagating calcium waves. *Cell calcium* **14**, 691-697, doi:10.1016/0143-4160(93)90095-n (1993).

83 Mikoshiba, K. IP3 receptor/Ca2+ channel: from discovery to new signaling concepts. *Journal of neurochemistry* **102**, 1426-1446, doi:10.1111/j.1471-4159.2007.04825.x (2007).

84 Hirata, M., Suematsu, E., Hashimoto, T., Hamachi, T. & Koga, T. Release of Ca2+ from a non-mitochondrial store site in peritoneal macrophages treated with saponin by inositol 1,4,5-trisphosphate. *The Biochemical journal* **223**, 229-236, doi:10.1042/bj2230229 (1984).

85 Iino, M. Biphasic Ca2+ dependence of inositol 1,4,5-trisphosphate-induced Ca release in smooth muscle cells of the guinea pig taenia caeci. *The Journal of general physiology* **95**, 1103-1122, doi:10.1085/jgp.95.6.1103 (1990).

86 Missiaen, L., Taylor, C. W. & Berridge, M. J. Luminal Ca2+ promoting spontaneous Ca2+ release from inositol trisphosphate-sensitive stores in rat hepatocytes. *The Journal of physiology* **455**, 623-640, doi:10.1113/jphysiol.1992.sp019319 (1992).

87 Smith, J. B., Smith, L. & Higgins, B. L. Temperature and nucleotide dependence of calcium release by myo-inositol 1,4,5-trisphosphate in cultured vascular smooth muscle cells. *The Journal of biological chemistry* **260**, 14413-14416 (1985).

88 Bezprozvanny, I. & Ehrlich, B. E. ATP modulates the function of inositol 1,4,5-trisphosphate-gated channels at two sites. *Neuron* **10**, 1175-1184, doi:10.1016/0896-6273(93)90065-y (1993).

89 Lu, J. P., Wang, Y., Sliter, D. A., Pearce, M. M. & Wojcikiewicz, R. J. RNF170 protein, an endoplasmic reticulum membrane ubiquitin ligase, mediates inositol 1,4,5-trisphosphate receptor ubiquitination and degradation. *The Journal of biological chemistry* **286**, 24426-24433, doi:10.1074/jbc.M111.251983 (2011).

90 Wright, F. A. & Wojcikiewicz, R. J. Chapter 4 - Inositol 1,4,5-Trisphosphate Receptor Ubiquitination. *Progress in molecular biology and translational science* **141**, 141-159, doi:10.1016/bs.pmbts.2016.02.004 (2016).

91 Patergnani, S. *et al.* Calcium signaling around Mitochondria Associated Membranes (MAMs). *Cell communication and signaling : CCS* **9**, 19, doi:10.1186/1478-811X-9-19 (2011).

92 Marchi, S. *et al.* Mitochondrial and endoplasmic reticulum calcium homeostasis and cell death. *Cell calcium* **69**, 62-72, doi:10.1016/j.ceca.2017.05.003 (2018).

93 Rizzuto, R., Brini, M., Murgia, M. & Pozzan, T. Microdomains with high Ca2+ close to IP3-sensitive channels that are sensed by neighboring mitochondria. *Science* **262**, 744-747, doi:10.1126/science.8235595 (1993).

94 Csordas, G., Thomas, A. P. & Hajnoczky, G. Quasi-synaptic calcium signal transmission between endoplasmic reticulum and mitochondria. *The EMBO journal* **18**, 96-108, doi:10.1093/emboj/18.1.96 (1999).

95 Rizzuto, R. *et al.* Close contacts with the endoplasmic reticulum as determinants of mitochondrial Ca2+ responses. *Science* **280**, 1763-1766, doi:10.1126/science.280.5370.1763 (1998).

96 Marchi, S. & Pinton, P. Alterations of calcium homeostasis in cancer cells. *Current opinion in pharmacology* **29**, 1-6, doi:10.1016/j.coph.2016.03.002 (2016).

97 Saris, N. E. & Carafoli, E. A historical review of cellular calcium handling, with emphasis on mitochondria. *Biochemistry. Biokhimiia* **70**, 187-194, doi:10.1007/s10541-005-0100-9 (2005).

98 Rizzuto, R., Simpson, A. W., Brini, M. & Pozzan, T. Rapid changes of mitochondrial Ca2+ revealed by specifically targeted recombinant aequorin. *Nature* **358**, 325-327, doi:10.1038/358325a0 (1992).

99 Palmer, A. E. & Tsien, R. Y. Measuring calcium signaling using genetically targetable fluorescent indicators. *Nature protocols* **1**, 1057-1065, doi:10.1038/nprot.2006.172 (2006).

100 Bock, F. J. & Tait, S. W. G. Mitochondria as multifaceted regulators of cell death. *Nature reviews. Molecular cell biology*, doi:10.1038/s41580-019-0173-8 (2019).

101 Mitchell, P. Chemiosmotic coupling in oxidative and photosynthetic phosphorylation. *Biological reviews of the Cambridge Philosophical Society* **41**, 445-502, doi:10.1111/j.1469-185x.1966.tb01501.x (1966).

102 Mitchell, P. Chemiosmotic coupling in oxidative and photosynthetic phosphorylation. 1966. *Biochimica et biophysica acta* **1807**, 1507-1538, doi:10.1016/j.bbabio.2011.09.018 (2011).

103 Bragadin, M., Pozzan, T. & Azzone, G. F. Kinetics of Ca2+ carrier in rat liver mitochondria. *Biochemistry* **18**, 5972-5978, doi:10.1021/bi00593a033 (1979).

104 De Stefani, D., Raffaello, A., Teardo, E., Szabo, I. & Rizzuto, R. A forty-kilodalton protein of the inner membrane is the mitochondrial calcium uniporter. *Nature* **476**, 336-340, doi:10.1038/nature10230 (2011).

105 Baughman, J. M. *et al.* Integrative genomics identifies MCU as an essential component of the mitochondrial calcium uniporter. *Nature* **476**, 341-345, doi:10.1038/nature10234 (2011).

106 Marchi, S. & Pinton, P. The mitochondrial calcium uniporter complex: molecular components, structure and physiopathological implications. *The Journal of physiology* **592**, 829-839, doi:10.1113/jphysiol.2013.268235 (2014).

107 Perocchi, F. *et al.* MICU1 encodes a mitochondrial EF hand protein required for Ca(2+) uptake. *Nature* **467**, 291-296, doi:10.1038/nature09358 (2010).

108 Mallilankaraman, K. *et al.* MCUR1 is an essential component of mitochondrial Ca2+ uptake that regulates cellular metabolism. *Nature cell biology* **14**, 1336-1343, doi:10.1038/ncb2622 (2012).

109 Moreau, B., Nelson, C. & Parekh, A. B. Biphasic regulation of mitochondrial Ca2+ uptake by cytosolic Ca2+ concentration. *Current biology : CB* **16**, 1672-1677, doi:10.1016/j.cub.2006.06.059 (2006).

110 Rimessi, A., Giorgi, C., Pinton, P. & Rizzuto, R. The versatility of mitochondrial calcium signals: from stimulation of cell metabolism to induction of cell death. *Biochimica et biophysica acta* **1777**, 808-816, doi:10.1016/j.bbabio.2008.05.449 (2008).

111 Green, D. R. & Llambi, F. Cell Death Signaling. *Cold Spring Harbor perspectives in biology* **7**, doi:10.1101/cshperspect.a006080 (2015).

112 Kroemer, G. *et al.* Classification of cell death: recommendations of the Nomenclature Committee on Cell Death 2009. *Cell death and differentiation* **16**, 3-11, doi:10.1038/cdd.2008.150 (2009).

113 Singh, R., Letai, A. & Sarosiek, K. Regulation of apoptosis in health and disease: the balancing act of BCL-2 family proteins. *Nature reviews. Molecular cell biology* **20**, 175-193, doi:10.1038/s41580-018-0089-8 (2019).

114 Galluzzi, L., Blomgren, K. & Kroemer, G. Mitochondrial membrane permeabilization in neuronal injury. *Nature reviews. Neuroscience* **10**, 481-494, doi:10.1038/nrn2665 (2009).

115 Danial, N. N. & Korsmeyer, S. J. Cell death: critical control points. *Cell* **116**, 205-219, doi:10.1016/s0092-8674(04)00046-7 (2004).

116 Li, Y. *et al.* Mechanistic insights into caspase-9 activation by the structure of the apoptosome holoenzyme. *Proceedings of the National Academy of Sciences of the United States of America* **114**, 1542-1547, doi:10.1073/pnas.1620626114 (2017).

117 Riedl, S. J. & Salvesen, G. S. The apoptosome: signalling platform of cell death. *Nature reviews. Molecular cell biology* **8**, 405-413, doi:10.1038/nrm2153 (2007).

118 Ravagnan, L., Roumier, T. & Kroemer, G. Mitochondria, the killer organelles and their weapons. *Journal of cellular physiology* **192**, 131-137, doi:10.1002/jcp.10111 (2002).

119 Giorgi, C., Romagnoli, A., Pinton, P. & Rizzuto, R. Ca2+ signaling, mitochondria and cell death. *Current molecular medicine* **8**, 119-130, doi:10.2174/156652408783769571 (2008).

120 Kroemer, G., Galluzzi, L. & Brenner, C. Mitochondrial membrane permeabilization in cell death. *Physiological reviews* **87**, 99-163, doi:10.1152/physrev.00013.2006 (2007).

121 Green, D. R. & Kroemer, G. The pathophysiology of mitochondrial cell death. *Science* **305**, 626-629, doi:10.1126/science.1099320 (2004).

122 Berridge, M. J., Bootman, M. D. & Roderick, H. L. Calcium signalling: dynamics, homeostasis and remodelling. *Nature reviews. Molecular cell biology* **4**, 517-529, doi:10.1038/nrm1155 (2003).

123 Rizzuto, R. & Pozzan, T. When calcium goes wrong: genetic alterations of a ubiquitous signaling route. *Nature genetics* **34**, 135-141, doi:10.1038/ng0603-135 (2003).

124 Cheng, H. P., Wei, S., Wei, L. P. & Verkhratsky, A. Calcium signaling in physiology and pathophysiology. *Acta pharmacologica Sinica* **27**, 767-772, doi:10.1111/j.1745-7254.2006.00399.x (2006).

125 Pinton, P., Giorgi, C., Siviero, R., Zecchini, E. & Rizzuto, R. Calcium and apoptosis: ER-mitochondria Ca2+ transfer in the control of apoptosis. *Oncogene* **27**, 6407-6418, doi:10.1038/onc.2008.308 (2008).

126 Sugawara, H., Kurosaki, M., Takata, M. & Kurosaki, T. Genetic evidence for involvement of type 1, type 2 and type 3 inositol 1,4,5-trisphosphate receptors in signal transduction through the B-cell antigen receptor. *The EMBO journal* **16**, 3078-3088, doi:10.1093/emboj/16.11.3078 (1997).

127 Jayaraman, T. & Marks, A. R. T cells deficient in inositol 1,4,5-trisphosphate receptor are resistant to apoptosis. *Molecular and cellular biology* **17**, 3005-3012, doi:10.1128/mcb.17.6.3005 (1997).

128 Mendes, C. C. *et al.* The type III inositol 1,4,5-trisphosphate receptor preferentially transmits apoptotic Ca2+ signals into mitochondria. *The Journal of biological chemistry* **280**, 40892-40900, doi:10.1074/jbc.M506623200 (2005).

129 Pinton, P. *et al.* Reduced loading of intracellular Ca(2+) stores and downregulation of capacitative Ca(2+) influx in Bcl-2-overexpressing cells. *The Journal of cell biology* **148**, 857-862, doi:10.1083/jcb.148.5.857 (2000).

130 Pinton, P. *et al.* The Ca2+ concentration of the endoplasmic reticulum is a key determinant of ceramide-induced apoptosis: significance for the molecular mechanism of Bcl-2 action. *The EMBO journal* **20**, 2690-2701, doi:10.1093/emboj/20.11.2690 (2001).

131 Roderick, H. L. & Cook, S. J. Ca2+ signalling checkpoints in cancer: remodelling Ca2+ for cancer cell proliferation and survival. *Nature reviews. Cancer* **8**, 361-375, doi:10.1038/nrc2374 (2008).

132 Scorrano, L. *et al.* BAX and BAK regulation of endoplasmic reticulum Ca2+: a control point for apoptosis. *Science* **300**, 135-139, doi:10.1126/science.1081208 (2003).

133 Vervliet, T., Parys, J. B. & Bultynck, G. Bcl-2 and FKBP12 bind to IP3 and ryanodine receptors at overlapping sites: the complexity of protein-protein interactions for channel regulation. *Biochemical Society transactions* **43**, 396-404, doi:10.1042/BST20140298 (2015).

134 Szado, T. *et al.* Phosphorylation of inositol 1,4,5-trisphosphate receptors by protein kinase B/Akt inhibits Ca2+ release and apoptosis. *Proceedings of the National Academy of Sciences of the United States of America* **105**, 2427-2432, doi:10.1073/pnas.0711324105 (2008).

135 Marchi, S. *et al.* Akt kinase reducing endoplasmic reticulum Ca2+ release protects cells from Ca2+-dependent apoptotic stimuli. *Biochemical and biophysical research communications* **375**, 501-505, doi:10.1016/j.bbrc.2008.07.153 (2008).

136 Kuchay, S. *et al.* PTEN counteracts FBXL2 to promote IP3R3- and Ca(2+)-mediated apoptosis limiting tumour growth. *Nature* **546**, 554-558, doi:10.1038/nature22965 (2017).

137 Bononi, A. *et al.* BAP1 regulates IP3R3-mediated Ca(2+) flux to mitochondria suppressing cell transformation. *Nature* **546**, 549-553, doi:10.1038/nature22798 (2017).

138 Tu, Y. *et al.* The Ubiquitin Proteasome Pathway (UPP) in the regulation of cell cycle control and DNA damage repair and its implication in tumorigenesis. *International journal of clinical and experimental pathology* **5**, 726-738 (2012).

139 Varshavsky, A. The Ubiquitin System, Autophagy, and Regulated Protein Degradation. *Annual review of biochemistry* **86**, 123-128, doi:10.1146/annurev-biochem-061516-044859 (2017).

140 Mani, A. & Gelmann, E. P. The ubiquitin-proteasome pathway and its role in cancer. *Journal of clinical oncology : official journal of the American Society of Clinical Oncology* **23**, 4776-4789, doi:10.1200/JCO.2005.05.081 (2005).

141 Goldstein, G. *et al.* Isolation of a polypeptide that has lymphocyte-differentiating properties and is probably represented universally in living cells. *Proceedings of the National Academy of Sciences of the United States of America* **72**, 11-15, doi:10.1073/pnas.72.1.11 (1975).

142 Ardley, H. C. & Robinson, P. A. E3 ubiquitin ligases. *Essays in biochemistry* **41**, 15-30, doi:10.1042/EB0410015 (2005).

143 Nasu, M. *et al.* High Incidence of Somatic BAP1 alterations in sporadic malignant mesothelioma. *Journal of thoracic oncology : official publication of the International Association for the Study of Lung Cancer* **10**, 565-576, doi:10.1097/JTO.0000000000000471 (2015).

144 Patergnani, S. *et al.* The endoplasmic reticulum mitochondrial calcium cross talk is downregulated in malignant pleural mesothelioma cells and plays a critical role in apoptosis inhibition. *Oncotarget* **6**, 23427-23444, doi:10.18632/oncotarget.4370 (2015).

145 Giorgi, C., Danese, A., Missiroli, S., Patergnani, S. & Pinton, P. Calcium Dynamics as a Machine for Decoding Signals. *Trends in cell biology* **28**, 258-273, doi:10.1016/j.tcb.2018.01.002 (2018).

146 Singh, S. S. *et al.* Dual role of autophagy in hallmarks of cancer. *Oncogene* **37**, 1142-1158, doi:10.1038/s41388-017-0046-6 (2018).

147 Missiroli, S. *et al.* PML at Mitochondria-Associated Membranes Is Critical for the Repression of Autophagy and Cancer Development. *Cell reports* **16**, 2415-2427, doi:10.1016/j.celrep.2016.07.082 (2016).

148 He, C. & Klionsky, D. J. Regulation mechanisms and signaling pathways of autophagy. *Annual review of genetics* **43**, 67-93, doi:10.1146/annurev-genet-102808-114910 (2009).

149 Xie, Z. & Klionsky, D. J. Autophagosome formation: core machinery and adaptations. *Nature cell biology* **9**, 1102-1109, doi:10.1038/ncb1007-1102 (2007).

150 Seglen, P. O. & Bohley, P. Autophagy and other vacuolar protein degradation mechanisms. *Experientia* **48**, 158-172, doi:10.1007/bf01923509 (1992).

151 Ji, C. H. & Kwon, Y. T. Crosstalk and Interplay between the Ubiquitin-Proteasome System and Autophagy. *Molecules and cells* **40**, 441-449, doi:10.14348/molcells.2017.0115 (2017).

152 Mizushima, N. & Komatsu, M. Autophagy: renovation of cells and tissues. *Cell* **147**, 728-741, doi:10.1016/j.cell.2011.10.026 (2011).

153 Cuervo, A. M. & Wong, E. Chaperone-mediated autophagy: roles in disease and aging. *Cell research* **24**, 92-104, doi:10.1038/cr.2013.153 (2014).

154 Feng, Y., He, D., Yao, Z. & Klionsky, D. J. The machinery of macroautophagy. *Cell research* **24**, 24-41, doi:10.1038/cr.2013.168 (2014).

155 Tsukada, M. & Ohsumi, Y. Isolation and characterization of autophagy-defective mutants of Saccharomyces cerevisiae. *FEBS letters* **333**, 169-174, doi:10.1016/0014-5793(93)80398-e (1993).

156 Klionsky, D. J. Autophagy: from phenomenology to molecular understanding in less than a decade. *Nature reviews. Molecular cell biology* **8**, 931-937, doi:10.1038/nrm2245 (2007).

157 Itakura, E. & Mizushima, N. Atg14 and UVRAG: mutually exclusive subunits of mammalian Beclin 1-PI3K complexes. *Autophagy* **5**, 534-536, doi:10.4161/auto.5.4.8062 (2009).

158 Ichimura, Y. *et al.* A ubiquitin-like system mediates protein lipidation. *Nature* **408**, 488-492, doi:10.1038/35044114 (2000).

159 Klionsky, D. J. *et al.* Guidelines for the use and interpretation of assays for monitoring autophagy (3rd edition). *Autophagy* **12**, 1-222, doi:10.1080/15548627.2015.1100356 (2016).

160 Lamark, T., Svenning, S. & Johansen, T. Regulation of selective autophagy: the p62/SQSTM1 paradigm. *Essays in biochemistry* **61**, 609-624, doi:10.1042/EBC20170035 (2017).

161 Stromhaug, P. E. & Seglen, P. O. Evidence for acidity of prelysosomal autophagic/endocytic vacuoles (amphisomes). *The Biochemical journal* **291 (Pt 1)**, 115-121, doi:10.1042/bj2910115 (1993).

162 Kaur, J. & Debnath, J. Autophagy at the crossroads of catabolism and anabolism. *Nature reviews. Molecular cell biology* **16**, 461-472, doi:10.1038/nrm4024 (2015).

163 Hosokawa, N. *et al.* Nutrient-dependent mTORC1 association with the ULK1-Atg13-FIP200 complex required for autophagy. *Molecular biology of the cell* **20**, 1981-1991, doi:10.1091/mbc.E08-12-1248 (2009).

164 Kim, J., Kundu, M., Viollet, B. & Guan, K. L. AMPK and mTOR regulate autophagy through direct phosphorylation of Ulk1. *Nature cell biology* **13**, 132-141, doi:10.1038/ncb2152 (2011).

165 Mizushima, N., Levine, B., Cuervo, A. M. & Klionsky, D. J. Autophagy fights disease through cellular self-digestion. *Nature* **451**, 1069-1075, doi:10.1038/nature06639 (2008).

166 Ravikumar, B. *et al.* Regulation of mammalian autophagy in physiology and pathophysiology. *Physiological reviews* **90**, 1383-1435, doi:10.1152/physrev.00030.2009 (2010).

167 Echeverry, N. *et al.* Inhibition of autophagy sensitizes malignant pleural mesothelioma cells to dual PI3K/mTOR inhibitors. *Cell death & disease* **6**, e1757, doi:10.1038/cddis.2015.124 (2015).

168 Sheikholeslami, K. *et al.* Simvastatin Induces Apoptosis in Medulloblastoma Brain Tumor Cells via Mevalonate Cascade Prenylation Substrates. *Cancers* **11**, doi:10.3390/cancers11070994 (2019).

169 Hwang, K. E. *et al.* Inhibition of autophagy potentiates pemetrexed and simvastatin-induced apoptotic cell death in malignant mesothelioma and non-small cell lung cancer cells. *Oncotarget* **6**, 29482-29496, doi:10.18632/oncotarget.5022 (2015).

170 Yoshikawa, Y. *et al.* High-density array-CGH with targeted NGS unmask multiple noncontiguous minute deletions on chromosome 3p21 in mesothelioma. *Proceedings of the National Academy of Sciences of the United States of America* **113**, 13432-13437, doi:10.1073/pnas.1612074113 (2016).

171 Rossi, M. *et al.* High throughput screening for inhibitors of the HECT ubiquitin E3 ligase ITCH identifies antidepressant drugs as regulators of autophagy. *Cell death & disease* **5**, e1203, doi:10.1038/cddis.2014.113 (2014).

172 Rybstein, M. D., Bravo-San Pedro, J. M., Kroemer, G. & Galluzzi, L. The autophagic network and cancer. *Nature cell biology* **20**, 243-251, doi:10.1038/s41556-018-0042-2 (2018).

173 Poklepovic, A. & Gewirtz, D. A. Outcome of early clinical trials of the combination of hydroxychloroquine with chemotherapy in cancer. *Autophagy* **10**, 1478-1480, doi:10.4161/auto.29428 (2014).

174 Park, J. *et al.* Haloperidol and clozapine block formation of autophagolysosomes in rat primary neurons. *Neuroscience* **209**, 64-73, doi:10.1016/j.neuroscience.2012.02.035 (2012).

175 Rossi, M. *et al.* Desmethylclomipramine induces the accumulation of autophagy markers by blocking autophagic flux. *Journal of cell science* **122**, 3330-3339, doi:10.1242/jcs.048181 (2009).

176 Bonora, M. *et al.* Subcellular calcium measurements in mammalian cells using jellyfish photoprotein aequorin-based probes. *Nature protocols* **8**, 2105-2118, doi:10.1038/nprot.2013.127 (2013).

177 Leestemaker, Y. *et al.* Proteasome Activation by Small Molecules. *Cell chemical biology* **24**, 725-736 e727, doi:10.1016/j.chembiol.2017.05.010 (2017).

178 Kania, E., Roest, G., Vervliet, T., Parys, J. B. & Bultynck, G. IP3 Receptor-Mediated Calcium Signaling and Its Role in Autophagy in Cancer. *Frontiers in oncology* **7**, 140, doi:10.3389/fonc.2017.00140 (2017).

179 Valladares, D. *et al.* IP3 receptor blockade restores autophagy and mitochondrial function in skeletal muscle fibers of dystrophic mice. *Biochimica et biophysica acta. Molecular basis of disease* **1864**, 3685-3695, doi:10.1016/j.bbadis.2018.08.042 (2018).

180 Carbone, M., Guo, Z. & Mao, W. Improving the Accuracy of Mesothelioma Diagnosis in China. *Journal of thoracic oncology : official publication of the International Association for the Study of Lung Cancer* **12**, e132, doi:10.1016/j.jtho.2017.04.020 (2017).

181 Carbone, M. *et al.* Positive nuclear BAP1 immunostaining helps differentiate non-small cell lung carcinomas from malignant mesothelioma. *Oncotarget* **7**, 59314-59321, doi:10.18632/oncotarget.10653 (2016).

182 Kushitani, K. *et al.* Immunohistochemical marker panels for distinguishing between epithelioid mesothelioma and lung adenocarcinoma. *Pathology international* **57**, 190-199, doi:10.1111/j.1440-1827.2007.02080.x (2007).

183 Szymiczek, A. *et al.* FTY720 inhibits mesothelioma growth in vitro and in a syngeneic mouse model. *Journal of translational medicine* **15**, 58, doi:10.1186/s12967-017-1158-z (2017).

184 Patergnani, S. *et al.* PRKCB/protein kinase C, beta and the mitochondrial axis as key regulators of autophagy. *Autophagy* **9**, 1367-1385, doi:10.4161/auto.25239 (2013).

185 Nicoli, F. *et al.* Naive CD8(+) T-Cells Engage a Versatile Metabolic Program Upon Activation in Humans and Differ Energetically From Memory CD8(+) T-Cells. *Frontiers in immunology* **9**, 2736, doi:10.3389/fimmu.2018.02736 (2018).

186 Gavioli, R., Vertuani, S. & Masucci, M. G. Proteasome inhibitors reconstitute the presentation of cytotoxic T-cell epitopes in Epstein-Barr virus-associated tumors. *International journal of cancer* **101**, 532-538, doi:10.1002/ijc.10653 (2002).

187 Greillier, L. & Astoul, P. Mesothelioma and asbestos-related pleural diseases. *Respiration; international review of thoracic diseases* **76**, 1-15, doi:10.1159/000127577 (2008).

188 Ying, S. *et al.* Serum HMGB1 as a Potential Biomarker for Patients with Asbestos-Related Diseases. *Disease markers* **2017**, 5756102, doi:10.1155/2017/5756102 (2017).

189 Xu, T., Jiang, L. & Wang, Z. The progression of HMGB1-induced autophagy in cancer biology. *OncoTargets and therapy* **12**, 365-377, doi:10.2147/OTT.S185876 (2019).